METEOR-Berichte

Oxygen and trace gases in the tropical southeastern Pacific

Cruise No. M90

October 28 – November 28, 2012
Cristobal (Panama) – Callao (Peru)

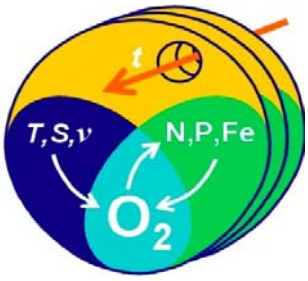

SFB 754

L. Stramma

Editorial Assistance:
DFG-Senatskommission für Ozeanographie
MARUM - Zentrum für Marine Umweltwissenschaften Bremen

2013

The METEOR-Berichte are published at irregular intervals. They are working papers for people who are occupied with the respective expedition and are intended as reports for the funding institutions. The opinions expressed in the METEOR-Berichte are only those of the authors.

The METEOR expeditions are funded by the *Deutsche Forschungsgemeinschaft (DFG)* and the *Bundesministerium für Bildung und Forschung (BMBF)*.

Editor:
DFG-Senatskommission für Ozeanographie
c/o MARUM – Zentrum für Marine Umweltwissenschaften
Universität Bremen
Leobener Strasse
28359 Bremen

Author:
Dr. Lothar Stramma
Physikalische Ozeanographie
GEOMAR
Düsternbrooker Weg 20
24105 Kiel, Germany

Telefon: +49 431-600 4103
Telefax: +49 431 600 4102
e-mail: lstramma@geomar.de

Citation: L. Stramma (2013) Oxygen and trace gases in the tropical southeastern Pacific - Cruise No. M90 – October 28 – November 28, 2012 – Cristobal (Panama) – Callao (Peru). METEOR-Berichte, M90, 40 pp., DFG-Senatskommission für Ozeanographie, DOI:10.2312/cr_m90

ISSN 2195-8475

Table of Content

1 Summary

During cruise M90 a combined chemical, physical oceanographic and biological research cruise was carried out in the eastern tropical Pacific in order to obtain a better understanding of the dynamics and variability of tropical oxygen minimum zones within the framework of the SFB 754 (Climate – Biogeochemical interactions in the tropical Oceans). The main goal of cruise M90 was the quantification of the longer periodic variability in the oxygen minimum zone of the tropical South Pacific. The longer periodic changes can be determined in comparison to earlier measurements made on the same sections. A special focus was on the role of large-scale circulation as well as the role of eddy processes for the changes in oxygen and the ventilation of the oxygen minimum zone.

The measurements on sections along 85°50'W, 6°S, 16°45'S and the survey of eddies included hydrographic measurements (CTD-rosette, ADCP), as well as oxygen, nutrients, stable isotope compositions of silicate and nitrate measurements. In addition nitrous oxide, short lived nitrogenous compounds and redox-sensitive species were measured to identify key microbial processes occurring in the Oxygen Minimum Zone (OMZ). The ADCP measurements with the 75 kHz and the 38 kHz ADCP provided good current measurements down to about 1200 m depth and were a good measurement component to identify the location of the eddies. All planned important measurements could be carried out and the survey of 3 eddies let to additional valuable data sets.

Zusammenfassung

Auf der Reise M90 wurde eine kombinierte chemische, physikalische und biologische Forschungsfahrt im östlichen tropischen Pazifik durchgeführt mit dem Ziel eines besseren Verständnisses der Dynamik und Variabilität der tropischen Sauerstoffminimum Zonen, die im Rahmen des SFB-754 (Klima-biogeochemische Wechselwirkungen im tropischen Ozean) durchgeführt wurde. Das Hauptziel auf der Reise M90 war die die Quantifizierung der längerperiodischen Variabilität in der Sauerstoffminimumzone des tropischen Südpazifiks. Die längerperiodischen Änderungen können im Vergleich zu früheren Messungen auf den Schnitten bestimmt werden. Ein besonderer Fokus lag auf der Rolle großräumiger Zirkulation als auch auf der Rolle von Wirbelprozessen für Sauerstoffänderungen und der Ventilation der Sauerstoffminimumzone.

Die Messungen auf Schnitten entlang 85°50'W, 6°S, 16°45'S und die Vermessung von Wirbeln beinhalteten hydrographische Messungen (CTD-Rosette, ADCP), sowie Messungen von Sauerstoff, Nährstoffen, stabilen Isotopenkomponenten von Silikat und Nitrat. Außerdem wurden Stickoxide, kurzlebige Stickstoffverbindungen und redox-sensitive Komponenten gemessen, um u.a. mikrobische Kernprozesse in der Sauerstoffminimumzone zu identifizieren. Die ADCP Messungen mit dem 75 kHz and dem 38 kHz ADCP lieferten gute Strömungsmessungen bis in ca. 1200 m Tiefe und waren eine gute Messkomponente um die Lage der Wirbel zu identifizieren. Alle geplanten wichtigen Messungen konnten durchgeführt werden und die Vermessung von 3 Wirbeln führt zu weiteren wertvollen Datensätzen.

2 Participants

Name	Discipline	Institution
Stramma, Lothar, Dr.	Chief scientist	GEOMAR
Arevalo Martinez, Damian	Nitrous oxide	GEOMAR
Baustian, Tina	Oxygen, nutrients	GEOMAR
Beltran Balarezo, Luis	Oceanogrography	IMARPE
Callbeck, Cameron	Nitrogen loss	MPI-Bremen
Charoenpong, Chawalit	N_2/Ar	UMass
Croot, Peter, Prof. Dr.	Redox tracer	NUIG
Daniel, Patrick	Biology	HMSSU
Dippe, Tina	ADCP/CTD-watch	GEOMAR
Döring, Kristin	Nitrogen, silicon	GEOMAR
Eirund, Gesa	Nitrogenous compounds	GEOMAR
Erbeck, Katrin	CTD watch	GEOMAR
Frank, Martin, Prof. Dr.	Silicon isotopes	GEOMAR
Garcia Diaz, Walter	Oceanography	IMARPE
Grasse, Patricia, Dr.	Nitrogen, silicon	GEOMAR
Hellemann, Dana	Microbial processes	IfAM
Höflich, Katharina	CTD watch	GEOMAR
Jonca, Justyna	O_2/PO_4 experiments	LEGOS
Komander-Hoepner, Sigrun	CTD watch	GEOMAR
Kretschmer, Kerstin	ADCP/CTD watch	GEOMAR
Link, Rudolf	CTD technician	GEOMAR
Lohmann, Martina	Oxygen, nutrients	GEOMAR
Lorenzo, Alberto	Chlorophyll	IMARPE
Martogli, Natascha	Microbial processes	IfAM
Mengis, Nadine	CTD processing	GEOMAR
Voigt, Janett	CTD watch	GEOMAR
Wuttig, Kathrin	Trace metals	GEOMAR
Hänsel, Carola	Meteorology	DWD
Frey, Bernd	Weather technician	DWD

GEOMAR
Helmholtz-Zentrum für Ozeanforschung Kiel
Düsternbrooker Weg 20
24105 Kiel / Germany
Internet: www.geomar.de
e-mail: info@geomar.de

IfAM
Institut für Allgemeine Mikrobiologie
Am Botanischen Garten 1-9
24118 Kiel / Germany
Internet: www.uni-kiel.de/mikrobio/
e-mail: rschmitz@ifam.uni-kiel.de

IMARPE
Instituto del Mar Peru
Esquina Gamarra y General Valle s/n
Chucuito – Calloa / Peru
Internet: www.imarpe.pe
e-mail: mgraco@gmail.com

LEGOS
Institut de Recherche pour le Développement
Research Unit "LEGOS"
UMR 5566 (CNES/CNRS/IRD/UPS)
18 avenue Edourd Belin
31401 Toulouse Cedex 9 / France
Internet: www.legos.obs-mip.fr
e-mail: aurelien.paulmier@legos.obs-mip.fr

MPI Bremen
Max-Planck Institute for Marine Microbiology
Celsiusstrasse 1 28359 Bremen / Germany
Internet: www.mpi.bremen.de
e-mail: glavik@mpi-bremen.de

NUIG
National University of Ireland Galway (NUIG)

School of Natural Sciences
Quadrangle Building, University Road
Galway / Ireland
Internet: www.nuigalway.ie
e-mail: peter.croot@nuigalway.ie

UMass
School of Marine Sciences and Technology
University of Massachusetts, Dartmouth
706 Rodney French Blvd
New Bedford, MA 02744-1221 / USA
Internet: www.umassd.edu
e-mail: maltabet@umassd.edu

HMSSU
Hopkins Marine Station
Stanford University, Gilly Lab
120 Oceanview Blvd.
Pacific Grove, CA 93950 / USA
Internet: www.gilly.stanford.edu
e-mail: lignje@stanford.edu

DWD
Deutscher Wetterdienst
Geschäftsfeld Seeschifffahrt
Bernhard-Nocht-Straße 76
20359 Hamburg / Germany
e-mail: seeschifffahrt@dwd.de
Internet: www.dwd.de

3 Research Program

The goal of cruise M90 was the quantification of the longer periodic variability in the oxygen minimum zone of the tropical South Pacific. The longer periodic changes can be determined in comparison to earlier measurements made on the same sections. A special focus was on the role of large-scale circulation as well as eddy processes for the changes in oxygen and the ventilation of the oxygen minimum zone.

Longer periodic variability of dissolved oxygen (DO) has been observed in tropical the oxygen minimum zones (OMZ) (Stramma et al. 2008) and was investigated on M90 in the tropical south-eastern Pacific. OMZ shoaling may restrict the usable habitat of fishes to a narrow surface layer (Stramma et al. 2012) and might lead to changes in the ecosystem influencing coastal economics.

The METEOR cruise M90 to the eastern tropical South Pacific Ocean was an effort of several groups of the DFG Collaborative Research Centre (SFB) 754. The goal of the study is the quantification of the longer periodic variability in the oxygen minimum zone of the tropical South Pacific with the special focus on the role of the large scale circulation as well as of eddy processes on the ventilation of the oxygen minimum zone.

On M90 a continuation of the large scale hydrographic (CTD-rosette) as well as current velocity (ADCP) measurements and three surveys of eddies were carried out. The aim was the determination of long-term variability and trends in hydrographic properties and circulation of the oxygen minimum zone with the focus on the oxygen supply paths in tropical region as well as the southern boundary of the oxygen minimum zone. Furthermore planned was a quantification of the oxygen distribution of an eddy for better estimates of lateral oxygen supply and ventilation of the oxygen minimum zone and an investigation of the variability of nutrient supply and utilisation (productivity) associated with eddies using stable Si and N isotope compositions of silicate and nitrate. Originally only the investigation of one cyclonic eddy was planned, but the investigation of 2 anticyclonic eddies and one cyclonic eddy let to a valuable additional data set.

In addition, nitrous oxide, short lived nitrogenous compounds and redox-sensitive species were measured e.g. to identify microbial key processes of the nitrogen cycle in the OMZ off Peru.

This cruise M90 is closely related to the shelf-near Pacific cruises M91 to M93. By combining the results from these cruises additional interaction between the different SFB-754 subprojects and a high degree of synergy is expected.

A plot of the station distribution (Figure 3.1) shows the large scale sampling and associated eddy survey measurements along the 16°45’S section. Originally Guayaquil was requested as start or end port. As the cruise started in Panama instead, we added a section at 6°S which lead to a closed box off Peru and we added 2 stations in the Panama 200 sm zone to extend the parameter measurements of Neodymium carried out in the equatorial and South Pacific during METEOR cruises M77/3 and M77/4 in early 2009 northward to the Panama Basin.

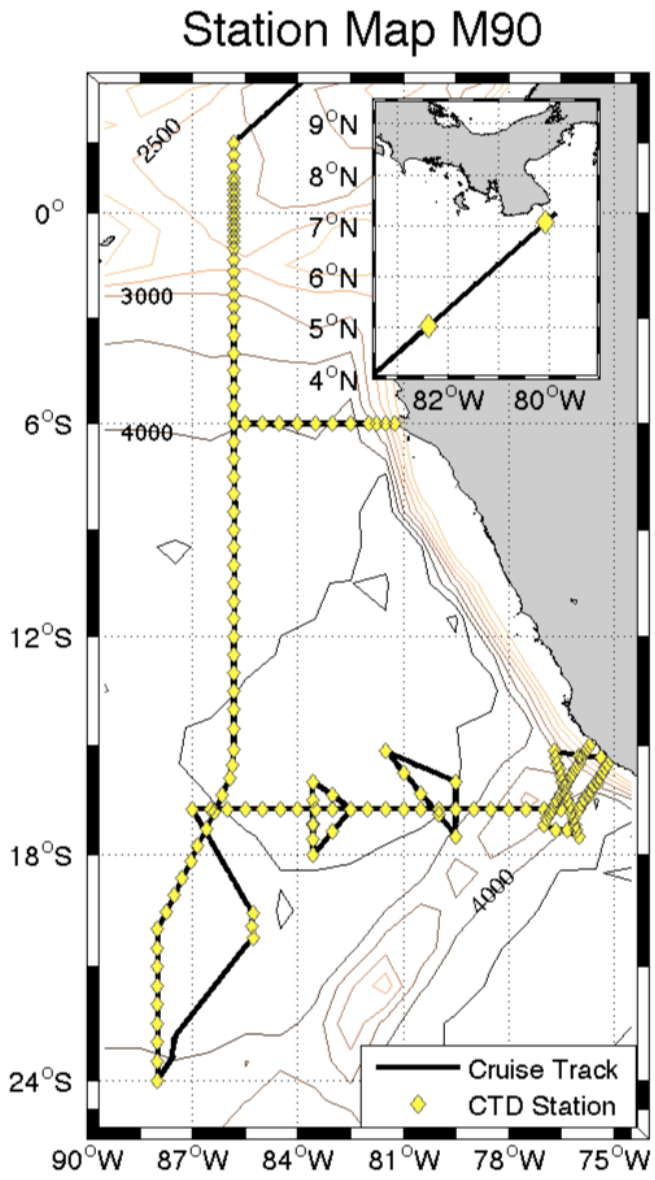

Fig. 3.1 Cruise track (black line) of METEOR cruise M90. Yellow (bright) squares show the CTD station locations.

4 Narrative of the Cruise

On 25 October 2012 METEOR called port in Cristobal, Panama. Two scientists arrived on METEOR ahead of the group from Panama City to be present when the 3 containers were placed on the dedicated locations for unpacking. Riots happened in the days before in Colon. These riots escalated on 26 October and the two scientists had to stay in their hotel until the evening for their security. The main scientific group traveled from Panama City to the ship on 27 October, fortunately no riots took place on this day and all scientific crew arrived safe on the ship. The containers were unpacked on 27 October and the instruments were arranged in the labs. In the afternoon of 28 October the pilot for the Panama Canal came on board,

however he had to leave again as the bunker boat arrived too late in the morning and bunkering was not completed in time. The passage through the Panama Canal began on 29 October in the evening. In the morning of 30 October METEOR loaded some lubricants for the engine off Balboa. Finally at 9:00 the transit to the first CTD station began about one day delayed. Two stations in the EEZ of Panama were carried out on October 30 and 31. During the earlier METEOR cruise M77/4 in 2009 Neodymium (Nd) isotopes were measured south of 2°N. As no Nd measurements existed before for the eastern North Pacific, this was a good opportunity to extend the data coverage of Nd towards Middle America. At the same time samples for concentration of REE's (rare earth elements) as well as for samples to be measured in the South Pacific were taken.

The section along 85°50'W covered before in 1993 and in 2009 was reached at 2°N in the afternoon of 1 November. To measure small scale changes in the equatorial channel, e.g. the Equatorial Undercurrent (EUC) the station spacing between 1°N and 1°S was reduced to 10 sm. The 85°50'W section was continued southward to 6°S reached in the evening of 4 November. To do measurements in a closed box in the eastern Pacific off Peru a section at 6°S measured in 2009 was measured again. The measurements along the section westwards started on 5 November following a transit to the Peruvian shelf from 85°50'W. The section along 6°S was finished on 7 November at 85°50'W and the 85°50'W section was investigated with CTD with bottle samples southward with a half degree station spacing. South of 15°30'S the southward section shifted gradually to 88°W at 20°S, to follow the track of the 1993 WOCE cruise to allow a direct comparison of the parameter distribution of both sections. The southernmost station on this section was made at 24°S on 13 November. From 24°S a transit followed to the region of the STRATUS mooring located at 19°56.3'S, 85°17.6'W.

On 15 November the 1994 WOCE section at 16°45'S was reached at 87°W and was measured eastward. However, one goal of the cruise M90 was to investigate eddies and eddies along the sections were measured with additional cross-sections. An anticyclonic eddy centered at about 83°30°W was crossed right in the middle on the 16°45'S section, and on 17 and 18 November a south-north section across the anticyclonic eddy was carried out. Afterwards the 16°45'S section was resumed eastward to 79°30'W, where a survey of a cyclonic eddy started on 19 November. The station work eastward along the 16°45'S section was resumed on 21 November and ended on 23 November on the Peruvian shelf.

An anticyclonic eddy was located here right of the coast centered at about 16°30'S, 76°30'W. From 24 November through the evening of 26 November two CTD sections with a station spacing of about 10 sm were made across this eddy. After a final ADCP section almost perpendicular at the cost at 15°S to 77°W FS METEOR was heading towards Callao, where the cruise M90 ended in the morning of 28 November 2012. On the transition between METEOR cruises M90 and M91 a reception was held on RV METEOR in the late afternoon of 29 November 2012 to present the ship and the goals of the Pacific legs M90 to M93 to the Peruvian authorities and Peruvian scientists.

5 Preliminary Results

In the following a detailed account of the types of observations, the methods and instrument used as well as some of the early results are given.

5.1 Hydrographic sampling

5.1.1 CTD system and salinity

(Nadine Mengis, Gerd Krahmann, Lothar Stramma, Rudi Link, Janett Voigt)

CTD-calibration

During M90 a total of 184 CTD-profiles were collected. The first set of casts for surveying the oxygen minimum layer was carried out to 1200 m depth and starting at CTD cast 95 to 1500 m depth. The final section CTD's 169 to 184 had again a target depth of 1200 m. In case the collected water volume was not enough for the biological and chemical analyses the cast was repeated to about 200 m depth. Occasionally, casts were carried out to full ocean depth (see station list).

Additionally to the normal setup of the CTD system an oxygen sensor manufactured by Rinko in Japan was attached to the system. Similar to the findings during cruise M83/1 we found the response time of this sensor to be slower than the regular Seabird sensors.

Data acquisition was done using Seabird Seasave software version 7.20b. The CTD was mounted on the GO4 rosette frame with a 24 bottle rosette sampling system with 10 l bottles. In varying configurations 23 to 24 bottles were attached to the rosette. On most profiles a configuration with 23 bottles was used, with one bottle removed for a PAR sensor. Deep ocean profiles were mostly done with 24 bottles as the PAR sensor had a maximum depth rating of 2000dbar. Due to cable problems in the beginning of the cruise the PAR Sensor was used only from cast #049 onward, regularly. From then on it had to be chosen, if either the PAR or the Altimeter was used, hence for shelf-near stations the PAR was not used, but the altimeter.

At cast #001 the second SBE Oxygen Sensor, showed far too low values compared to the primary sensor, which showed 100% saturation on the surface. Also at a depth of about 1120m there was a jump of the primary sensor. The second oxygen sensor did not show this behavior. Despite the too low values the second sensor was fine. The jump in the first oxygen sensor was due to an increasing noise building up in the first temperature sensor. This jump affected the salinity and the oxygen of the first sensor string. The second sensor string was fine. For the upcast there was no noise. For the next cast the primary temperature sensor was changed.

At cast #002 the second oxygen sensor still showed too low values but nevertheless was stable. At a depth of about 780m the first temperature sensor collapsed, hence the salinity and the oxygen calculations from the first sensor string are unusable. The second senor string was fine and used for the final calibration.

After cast #002 it was found that also the conductivity sensor had collapsed, hence the decision to exchange the complete CTD was appropriate. So from cast #003 on the GEOMAR SBE5 was used, see table 5.1 for more details on the sensors used and the serial numbers.

Before cast #064 the winch was exchanged. During the cast four fuses broke and the contact to the CTD was lost for some time. The program on board was restarted and the cast was set to #965. Later it was tried to put the two parts of the cast together in one profile. The winch was changed back.

At cast #081 the rosette carousel seemed to have a connection problem. Not all bottles that were fired closed and some were skipped by the program. When the water sampler came on

deck, it was not able to reconstruct which bottle was fired on which depth. The station was repeated, as cast #082.

The final calibration of the CTD data was done using the secondary set of sensors as it remained unchanged during the whole cruise.

Device	Model number	Serial number
CTD deck unit	SBE 11 plus	SN 11P22348-0530
CTD underwater unit	SBE 9 plus (**SBE04**)	SN 00P34783-0752
Pressure Sensor	Digiquarz	SN 89964
Pump, primary	SBE 5T	SN 4751
Pump, second	SBE 5T	SN 4749
Temperature, primary	SBE 3	SN 4875 (Profil 001) SN 4831 (Profil 002)
Temperature, second	SBE 3	SN 2814
Conductivity, primary	SBE 4	SN 3425
Conductivity, second	SBE 4	SN 3981
Oxygen, primary	SBE 43	SN 0145
Oxygen, second	SBE 43	SN 0985
Fluorescence and Turbidity	Wetlabs, FLNTU	SN 2294
Altimeter	Benthos/Teledyne	SN 42106
Oxygen	Rinko	SN 054
Underwater PAR	Biospherical	SN 4702

Device	Model number	Serial number
CTD deck unit	SBE 11 plus	SN 11P22348-0530
CTD underwater unit	SBE 9 plus (**SBE 05**)	SN 09P10108-0410
Pressure Sensor	Digiquarz	SN 61184
Pump, primary	SBE 5T	SN 2603
Pump, second	SBE 5T	SN 4375
Temperature, primary	SBE 3	SN 4673 (Profil 003 -)
Temperature, second	SBE 3	SN 4875
Conductivity, primary	SBE 4	SN 2512
Conductivity, second	SBE 4	SN 3366
Oxygen, primary	SBE 43	SN 1314
Oxygen, second	SBE 43	SN 0194
Fluorescence and Turbidity	Wetlabs, FLNTU	SN 2294
Altimeter	Benthos/Teledyne	SN 42106
Oxygen	Rinko	SN 054
Underwater PAR	Biospherical	SN 4702

Table 5.1 Sensors used for the SBE 04 (top) and the SBE 05 (bottom).

The GEOMAR Guildline Autosal salinometer #8 was used for CTD conductivity cell calibration (operated by J. Voigt and L. Stramma). The Guildline Autosal salinometer #5 was available as backup, but had not been used for measurements but only for a quick check. Calibration during operation was done in two ways: IAPSO Standard Seawater (P154, K15=0.99990) was measured at the beginning of the salinometer use. In addition, a so called

"substandard" (essentially a large volume of water with constant but unknown salinity), obtained 2 times from deep bottles from the CTD casts was used to track the stability of the system. The substandard showed that no drift appeared during the measurements. Hence the AS8 was stable during the entire measurement time as well as from one measurement day to the next. A short test of AS5 showed that the measurements were stable and the substandard used on AS8 was recorded with the same conductivity ratio right away without standardization of the AS5 instrument.

The conductivity calibration of the downcast data was performed using a linear fit with respect to conductivity, temperature, and pressure. For the first two profiles this resulted in the calibration: C_corrected = C_observed -0.0061039 + 1.0304e-06 * P + 0.00025692 * T + 0.0012315 * C. In difference to the usual procedure the upcast calibration result was used as the downcast calibration appeared to be problematic because of strong surface salinity variability during the 2 casts and because so few calibration measurements were available. Using 100% of the 10 samples for calibration a r.m.s. of 0.00076 S/m corresponding to a salinity of 0.0078 PSU was found for the upcast.

For the remaining 182 profiles the calibration was: C_corrected = C_observed -0.0053522 – 1.1934e-07 * P – 0.00019864 * T + 0.0019138 * C). Using 67% of the 256 samples for calibration a r.m.s. of 0.00009 S/m corresponding to a salinity of 0.0010 PSU was found for the downcast.

We chose the downcast as final dataset as: 1) Sensor hysteresis starts from a well defined point, and 2) the incoming flow is not perturbed by turbulence generated by the CTD-rosette.

5.1.2 Oxygen

(Tina Baustian, Gerd Krahmann, Nadine Mengis)

Oxygen measurements:

Samples for the determination of dissolved oxygen after Winkler (1888) were taken from a total of 51 CTD casts to calibrate the oxygen sensors (SBE 43) and to support chemical and biological CTD data. On a regular CTD cast, 17 to 23 depths between the surface and 1500 m were sampled for dissolved oxygen. Additionally, dissolved oxygen samples were collected on 11 casts deeper than 1500 m (deepest cast down to 5300 m), yielding a total of 1257 samples for the entire cruise.

The precision of the oxygen concentration measurements determined from the titration was 0,45 µmol/L (arithmetical average of all standard deviations) based on 112 replicate measurements with 2 – 4 replicates each.

To test if a higher accuracy could be reached when determining dissolved oxygen concentrations in very low oxygen water masses (below 10 µmol O_2/L), a second thiosulfate solution with a concentration of 0,002 mol/L was used in addition to the commonly used 0,02 mol/L thiosulfate solution. Four to six replicates were taken for a total of 8 samples, all taken within the center of the OMZ in water masses with less than 10 µmol O_2/L. For each sample, half of the replicates was titrated using the 0,002 mol/L thiosulfate solution and the other half using the 0,02 mol/L thiosulfate solution, and results were compared. However, when

performing the titration with the 0,002 mol/L thiosulfate solution, the exact equilibration point was very hard to detect, and there was no clear trend to a better accuracy.

The CTD oxygen sensor calibration was performed similarly to the conductivity calibration. As the sensors changed after the first two profiles, again two sets of calibration coefficients were derived. For the first two profiles with was again derived from the upcast as the few bottles taken for calibration appeared to create near surface problems. The resulting calibration correction for the secondary oxygen sensor was: o_corrected = o_observed (µmol/kg) + 14.379 – 0.033726 * P – 1.0149 * T + 2.1689 * O. Using 100% of the 12 samples for calibration a r.m.s. of 3.9 µmol O_2/kg was determined as uncertainty of the calibration.

The resulting calibration correction for the secondary oxygen sensor for profiles 3 to 184 was: o_corrected = o_observed (µmol/kg) + 1.0099 + 0.000893 * P – 0.091072 * T + 0.024136 * O. Using 67% of the 978 samples for calibration a r.m.s. of 0.68 µmol O_2/kg were determined as uncertainty of the calibration.

5.1.3 Nutrients

(Martina Lohmann)

Nutrients were measured on-board with a QuAAtro auto-analyzer from SEAL Analytical. The following methods from SEAL analytics were used:

Nitrite and Nitrate – Q-068-05 Rev 7; The nitrate is determined as nitrite after reduction on a cadmium coil. The nitrite is determined with a colorimetric metric method where sulphanilamide is forming a diazo compound. An example for the nitrite distribution is shown in figure 5.1.

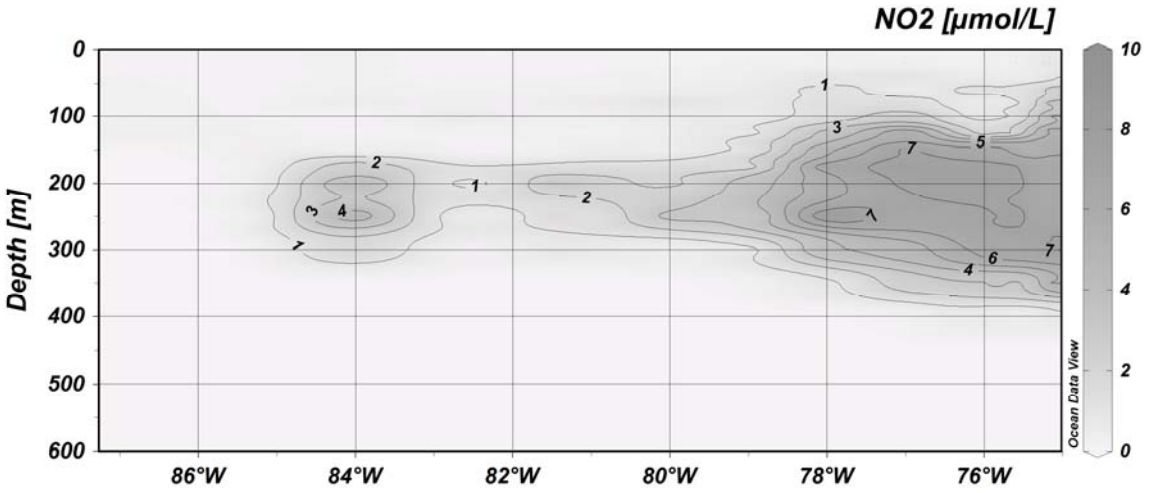

Fig. 5.1 Nitrite distribution along the 16°45'S section in µmol/L.

Phosphate – Q-064-05 Rev 4; this is the colorimetric method based on reaction with molybdate and antimony ions.

Silicate – Q-066-05 Rev 3; this is the colorimetric method where a silico-molybdate complex is reduced to molybdenum blue.
Samples from the CTD were measured on 1548 samples during the cruise.
The precision of the nutrient measurements were determined from triplicate samples taken at a selection of stations. The precisions of the measurements are determined to be: 0.1 µmol/L for nitrate, 0.02 µmol/L for phosphate and 0.24 µmol/L for silicate.
In addition to the CTD casts, nutrient samples were analyzed from underway measurements.

5.1.4 Current Observations

(Kerstin Kretschmer, Tina Dippe)

RV METEOR is equipped with a hull mounted RDI OceanSurveyor ADCP of 75 kHz and a sea-well mounted RDI OceanSurveyor ADCP of 38 kHz. For almost the entire cruise both were operative for underway current measurements.

However, in the beginning of the cruise time gaps within the data arose (see Figure 5.2) especially in the 75 kHz ADCP, while processing the velocity data. Those occurred mainly during the stations, since the bowthruster had to be used to stabilize the vessel. Therefore, we decided to stay on position without using the bowthruster for about five minutes after finishing the CTD-station. Nevertheless, the time gaps were still present, but did not have any effect on the spatial resolution of the current velocity measurements.

Navigational data directly available for the ADCP system was mostly supplied from the integrated SEAPATH-system: GPS-position and heading calculated from 2-dimensional GPS and gyros.

There was no synchro heading fed to the ADCP deck unit. In order to have more than one source of heading information and to have a consistent navigation data set, unprocessed heading output from the FibreOpticGyro as well as all other navigation systems was stored via the DAVISShip database.

To avoid acoustic interferences, it was also necessary to have the on-board 75 kHz Doppler Velocity Log as well as the Parasound switched off.

The OceanSurveyor 75 kHz recorded single pings, pinging ca. every 2.44 seconds in narrowband mode. The range was typically between 700 and 800m. The OceanSurveyor 38 kHz also recorded single pings, pinging ca. every 3.05 seconds in narrowband mode. The range was typically between 1400 and 1500m (Fig. 5.3).

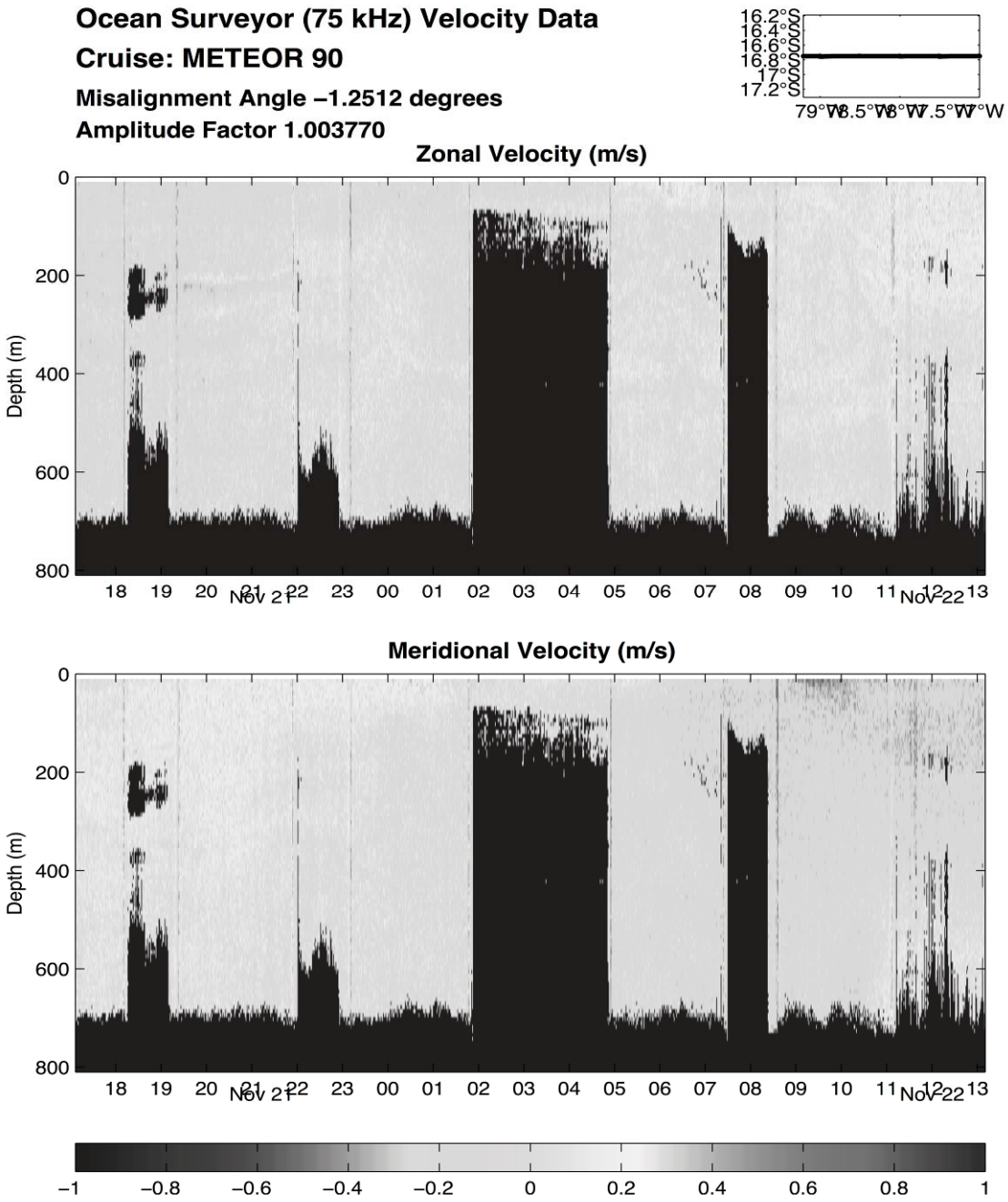

Fig. 5.2 Shipboard ADCP velocity data (75 kHz) versus time (UTC) along the 16°45'S section during 21st and 22nd November. The time gaps can be seen as vertical black patches.

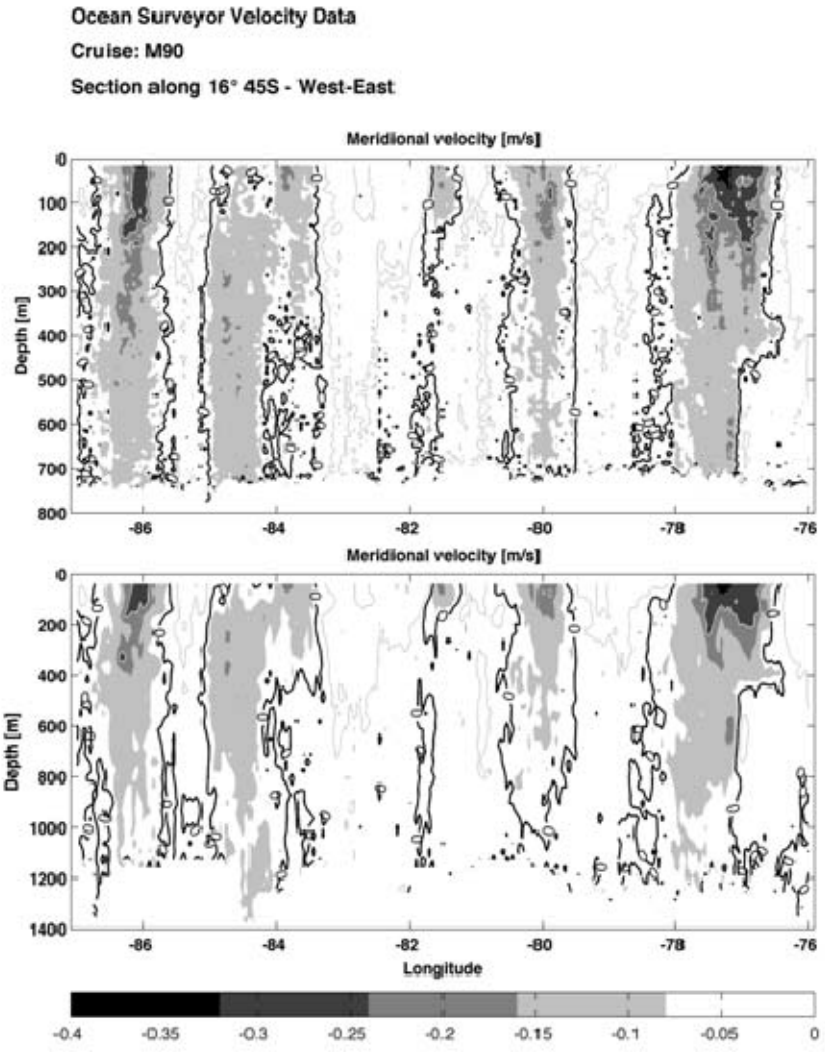

Fig. 5.3 Meridional velocity along the 16°45'S section of OceanSurveyor 75 kHz (top) and OceanSurveyor 38 kHz (bottom). The zero contour line is shown in black. The white and gray contour lines represent negative and positive velocities, respectively.

5.1.5 Hydrographic results

(Lothar Stramma, Nadine Mengis, Kerstin Kretschmer)

One objective of the RV METEOR cruise M90 was to map the distribution of the OMZ in relation to the water masses and currents in the eastern tropical Pacific in the context of the SFB-754. A new focus was the investigation of eddies and their influence on the OMZ. The temperature and salinity distribution of cyclonic and anticyclonic eddies in the eastern South Pacific has recently been described (Chaigneau et al. 2011), however the oxygen distribution as well as the chemical parameter distribution was widely unknown. When we repeated the 1994 WOCE line along 16°45’S we crossed two anticyclonic eddies in the open ocean at 85°30’W and 83°30’W, a cyclonic eddy at about 81°30’W and an anticyclonic eddy near the shelf at about 76°W (Fig. 5.4). We carried out cross-sections across the eddies centered at 83°30’W, 81°30’W and 76°W. All eddies showed clear signals in temperature, salinity,

density and oxygen. As an example the anticyclonic eddy near the shelf at 76°W is shown here.

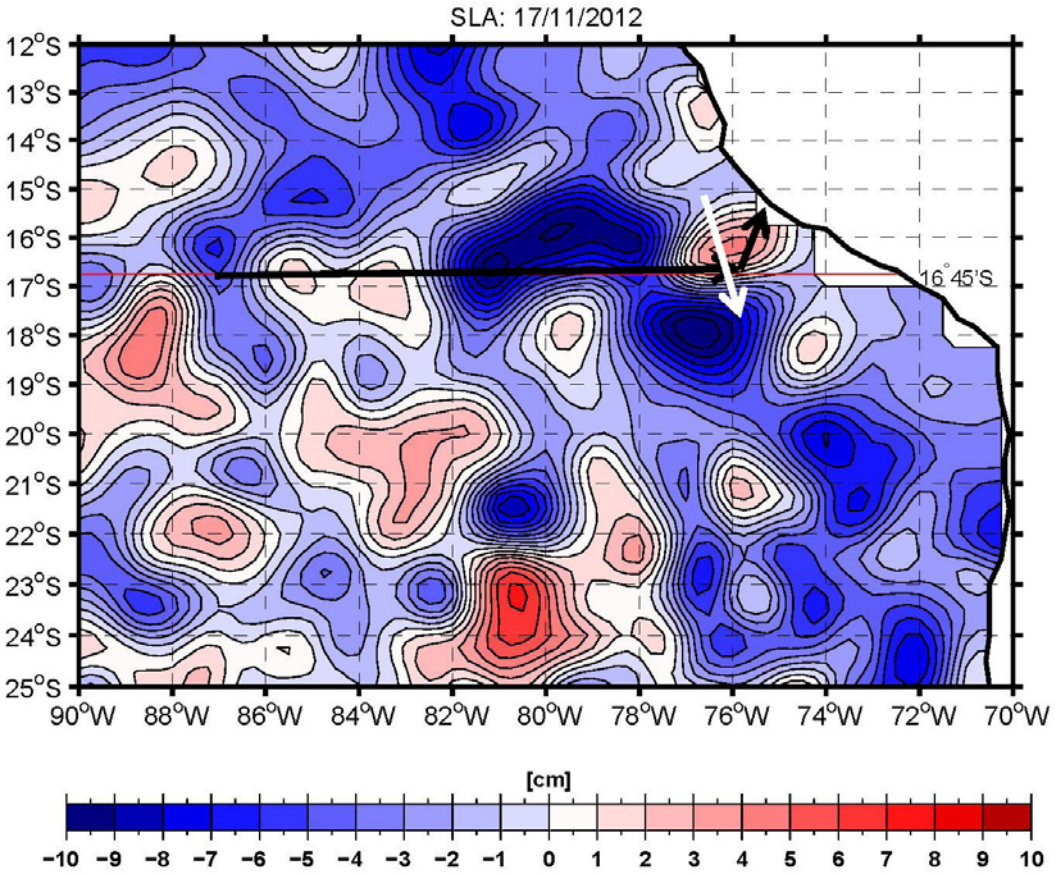

Fig. 5.4 AVISO sea surface height anomaly for 17 November 2012. The cruise track along the 16°45'S section is shown in black, the section across the anticyclonic eddy near the shelf in white. Anticyclonic eddies are red (bright), cyclonic eddies blue (dark).

Current measurements along the 16°45'S section reveal the presence of two anticyclonic and one cyclonic eddy (see Figure 5.4), which have been surveyed by several separate sections. The section across the anticyclonic eddy near the coast (Figure 5.5) shows the clear southwestward component in the northwestern part of the section and the northeastward component in the southeastern part, as typical for an anticyclonic circulation in the southern hemisphere.

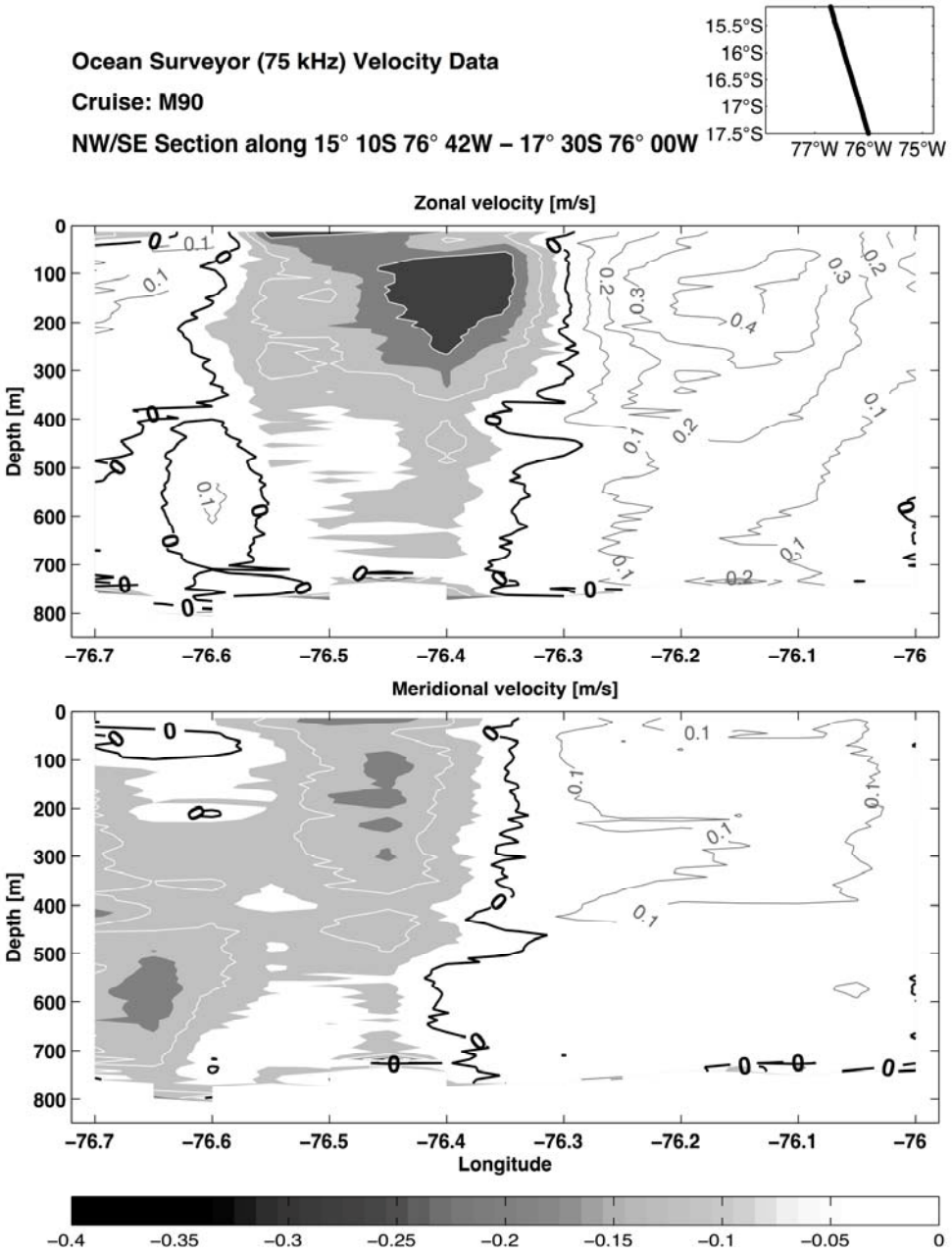

Fig. 5.5 Meridional and zonal velocity components of OceanSurveyor 75 kHz along the NW/SE section shown in the box at the top (15°10'S 76°42'W - 17°30'S 76°00'W). The zero contour line is shown in black. The white and gray contour lines represent negative and positive velocities, respectively.

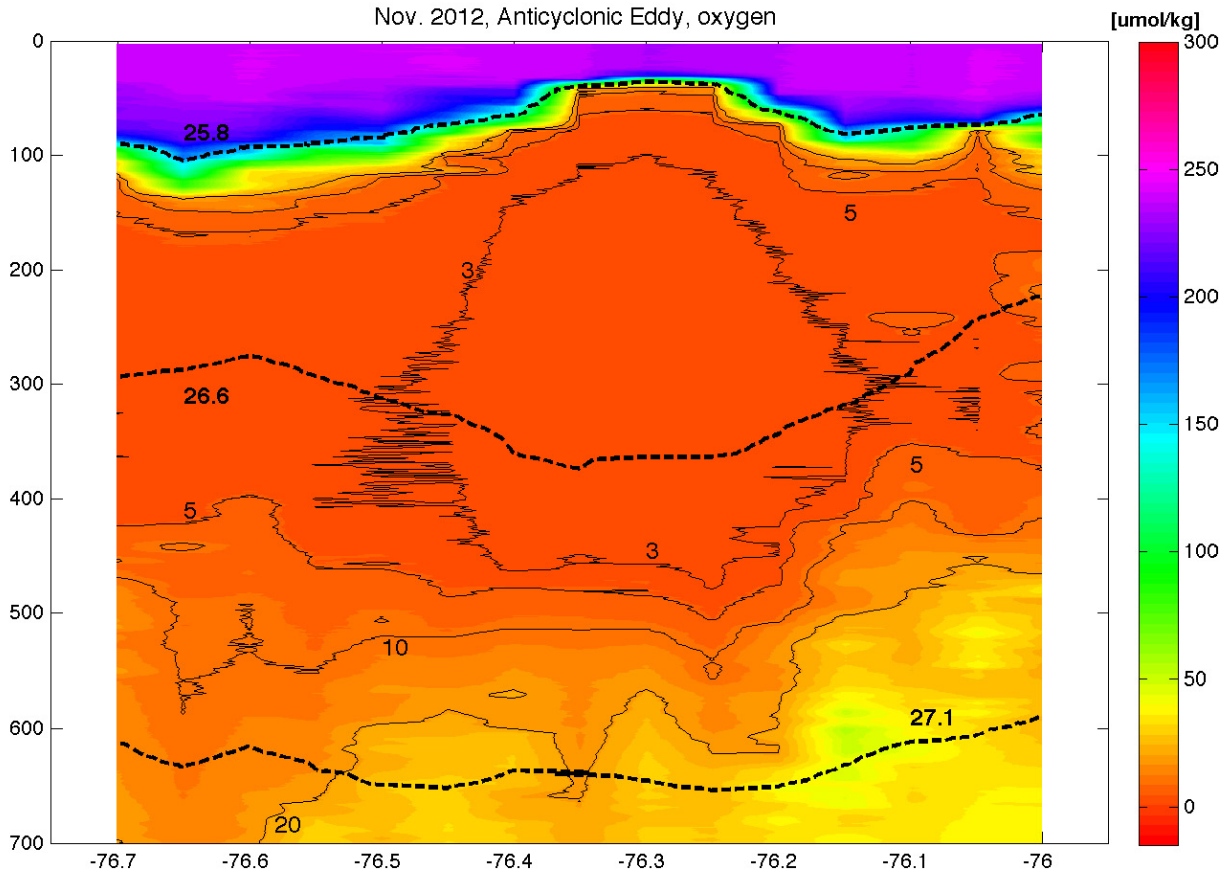

Fig. 5.6 Oxygen distribution (in µmol/kg) along the anticyclonic eddy from 15°10'S 76°42'W - 17°30'S 76°00'W. Included are some selected isopycnals (dashed black lines).

The related oxygen distribution along this section clearly shows a vertical extended minimum in the core of the anticyclonic eddy (Figure 5.6). The low oxygen layer reaches closer to the surface in the center of the eddy than in the surrounding water. The eddy has a large isolated core of water with dissolved oxygen content of less than 3 µmol/kg. Connected to the oxygen minimum are higher temperature and salinity values and a downwelling of the deeper isopycnals and an uprise of shallow isopycnals (Figure 5.6). Connected to the eddy is a layer of strong nitrite (Figure 5.1). According to measurements with a STOX sensor Thamdrup et al. (2012) described for the eastern Pacific, that nitrite only accumulates when oxygen is depleted below 50 nmol/kg. Hence the oxygen in the core of the anticyclonic eddy is even lower than measured with the CTD, as the CTD and the oxygen titration can't resolve such low oxygen values. The open question on eddies is how much these eddies influence the oxygen in the OMZ and a careful evaluation of the measured sections across the eddies will lead to a better understanding of the impact of eddies on the oxygen distribution.

5.2 Biogeochemical sampling

5.2.1 Crustal elements (Ti and Mn)

(Peter Croot, Kathrin Wuttig, Justyna Jonca)

For the previous expedition along 85°50' W (M77/4) a Class 100 clean container and trace metal clean GO-FLO bottles were used to sample for iron and other contamination prone elements. However for logistical reasons on this cruise, these facilities were unavailable and only sampling from the regular CTD was made, this meant a more restricted program for sampling of elements that are not contaminated by the Niskins of the CTD. For these reasons we focused on Mn and Ti, two tracers of crustal elements that indicate primarily processes of sediment input and aeolian input to the water column respectively. These are the first known shipboard measurements of Ti at sea in the Eastern Tropical South Pacific (ETSP). Mn was analyzed directly onboard using a spectrophotometric flow injection method. Unfortunately in the later stages of the cruise problems arose with the baseline and analysis was discontinued. Sampling for Mn however was continued and the archived samples will be analyzed upon return to the laboratory in Kiel. The early Mn results showed the presence of a secondary Mn maxima in the OMZ along the 85°50' W transect in more detail than was possible previously during M77/4.

Water samples were also taken at selected stations for later analysis back in the laboratory in Galway for the analysis of other trace metals (principally Cd and Ni). Further analysis of the Mn samples collected on this expedition will be performed in the laboratory in Kiel upon return of the samples.

5.2.2 Chromophoric Dissolved Organic Matter (CDOM)

(Peter Croot, Kathrin Wuttig, Justyna Jonca)

Samples from the CTD Niskins were filtered (0.2 μm Sarstedt) and analysed for CDOM absorbance and fluorescence. CDOM absorbance was measured using a 1 m pathlength liquid waveguide capillary cell (LWCC) coupled to an Ocean Optics USB4000 spectrophotometer. CDOM fluorescence was measured by obtaining 3D Excitation Emission Matrix (EEM) spectra using the new Aqualog (Horiba Scientific) fluorometer. EEMs are constructed from a matrix of measurements spanning a range of excitation and emission wavelengths. All spectra were corrected automatically for internal absorption and for Rayleigh scattering. Post processing of the data will be performed using PARAFAC (Parallel Factor Analysis) analysis with either the software supplied with the Aqualog (Special PARAFAC analysis software in the program SOLO) or via existing Matlab™ routines. All CDOM absorbance and fluorescence signals were normalized to ultrapure water supplied from a Direct 8 Milli-Q unit (Millipore).

Initial results onboard showed that vertical profiles of CDOM absorbance and fluorescence were typical of the open ocean with low absorbance but high spectral slopes coupled with low humic fluorescence (ex/em 320/420) in surface waters illustrating bleaching due to solar irradiation. In the OMZ humic fluorescence appeared to co-vary with the apparent oxygen utilization (AOU). During this expedition we also made the first comparison for measurements of humic abundance using two different analytical approaches; the EEM

method as described above and a voltammetric method utilizing the bromated catalyzed reduction signal of Fe-humic complexes. The CDOM data will be combined with the other data from this cruise to assess the role of reactive oxygen species (e.g. Oxygen and hydrogen peroxide) on the transformation of organic matter.

5.2.3 Redox sensitive species (Iodide, Fe(II), H_2O_2)

(Peter Croot, Kathrin Wuttig, Justyna Jonca)

The oxygen sensitive redox species of iron and iodine can be used as tracers of redox processes within the OMZ. A similar further tracer is the intermediate reduction product of O_2, H_2O_2 which is produced via photochemistry in the euphotic zone but in the OMZ may result from respiration or chemical oxidation processes.

During M90 we measured Fe(II) and H_2O_2 using a single flow injection instrument (Waterville Analytical) by splitting the reagent injection into two separate loops; in which each loop was optimized for the luminol chemiluminscence induced by Fe(II) and H_2O_2 respectively. A new flow cell and photon counter increased the sensitivity of this method relative to the instrument used previously on M77/4. However during M90 problems were encountered with the communication of the photon counter with the computer due to the necessity of using blue-tooth for this, while this did not affect the overall performance of the instrument it did lead to numerous data dropouts. In general H_2O_2 concentrations were dominated by surface irradiation with highest concentrations at the surface and in the mixed layer, with concentrations decreasing exponentially with depth. Smaller maxima were often found at the boundaries of the OMZ. At several offshore stations significant Fe(II) concentrations were found in the OMZ indicating the transport of reduced iron from the shelf or the redox transformation of iron in sinking particles. Along the East Pacific Rise (EPR) there was some indication of potential hydrothermal plumes as seen by small but significant Fe(II) concentrations at 1500 - 2000 m, a more full analysis for his data will take place once the dissolved Mn analysis is complete. High Fe(II) levels were encountered on the Peruvian shelf consistent with the flux of Fe(II) from the underlying sediments as seen previously.

The two inorganic redox species of iodine were measured directly onboard; Iodide (I^-) directly by voltammetry (Metrohm VA663 and μAutolab 3) and Iodate (IO_3^-) by spectrophotometry (10 cm pathlength cell with Ocean Optics USB4000 spectrophotometer) as I_3^- after reduction with sulfamic acid and the addition of 10% KI. During M90 we analyzed 7 stations for iodate and iodide, mostly along the 16°45'S transect, and typically found high iodide and low iodate concentrations in surface waters and in the OMZ. At stations on the coastal shelf there was some evidence for a flux of iodide from the sediments, as total inorganic iodine (TII= iodide + iodate) exceeded the amount predicted by the usual conservative behavior of iodine in seawater. An attempt was made to measure dissolved organic iodide (DOI) in the water column by UV irradiating water samples onboard and then detecting the total iodine as iodide, and determining DOI by difference from the sum of the TII. However due to the analytical difficulty of determining a statistically significant concentration difference between two large numbers this approach was not pursued further.

5.2.4 Nitrous oxide

(Damian Arevalo, Gesa Eirund)

The assessment of marine emissions of climate relevant gases has become a critical issue in the attempt to improve our current understanding of the impacts of the ocean on atmospheric chemistry and therefore, on climate. In order to examine the vertical distribution and sea to air fluxes of nitrous oxide (N_2O), a combination of discrete and continuous measurements has been employed during the M90 cruise. In addition, other potent greenhouse gases such as carbon monoxide and dioxide (CO and CO_2, respectively) were assessed.

N_2O depth profiles

A total of 30 stations were sampled between 2 to 16°S and 85° to 76°W with emphasis on the upper 1000 m of the water column. Bubble-free samples were collected in triplicates from 10 L Niskin bottles and subsequently a 10 mL headspace of helium and 50 µL of saturated mercuric chloride solution were added. After an equilibration period of at least 6 hours the headspace sample was measured by means of a gas chromatograph equipped with an electron capture detector (GC/ECD). The GC was calibrated on a daily basis using dilutions of a standard gas mixture. Additionally, depth profiles of hydroxylamine (an important short-lived intermediate compound in the nitrogen cycle) were achieved for selected stations after conversion of N_2O samples by means of the chemical method described by Kock (2011).

Underway measurements

An underway system (Fig. 5.7) was used to perform continuous measurements of oceanic and atmospheric nitrous oxide (N_2O), carbon monoxide (CO) and carbon dioxide (CO_2). It combines an OA-ICOS (off-axis integrated cavity output spectroscopy) analyzer from Los Gatos Research Inc. for N_2O and CO, a non-dispersive infrared analyzer from LI-COR Biosciences for CO_2 determinations and a Weiss type equilibrator. The water was drawn on board by using a submersible pump installed at the moonpool of the ship and was subsequently conducted at a rate of about 2 L min^{-1} through the equilibrator. A 200 mL sample of air was drawn from the headspace of the equilibrator and continuously pumped through the instruments and then back to the equilibration chamber forming a closed loop. The air stream was dried before being injected into the analyzers by means of a Nafion® tube in order to diminish interferences due to the water vapor content of the sample. The water temperature was constantly monitored by means of a high accuracy digital thermometer placed in the equilibrator. Ambient air measurements were accomplished by pumping air into the system from a suction point located at the ships mast at about 30 m high. Furthermore, control measurements and calibration procedures were performed every 24 h using two standard gas mixtures bracketing the expected concentrations and compressed air.

Discrete comparison samples for N_2O (Fig. 5.7) and CO_2 were carried out in 6 h intervals by sampling from the same water stream that fed the underway setup. N_2O samples were treated as explained above and measured on board with GC/ECD whereas DIC/TA samples were collected and stored to be measured at the Chemical Oceanography department of the

GEOMAR in Kiel. In addition, measurements of nutrients (nitrate, nitrite, phosphate and silicate) were performed on board by using a QuAAtro (Seal Analytical, Norderstedt, Germany) segmented flow analyzer. Filtered samples of seawater from the underway setup were also analyzed for cDOM in cooperation with Dr. P. Croot. Such measurements were performed in order to better understand the biogeochemical processes affecting dissolved gases in the surface ocean.

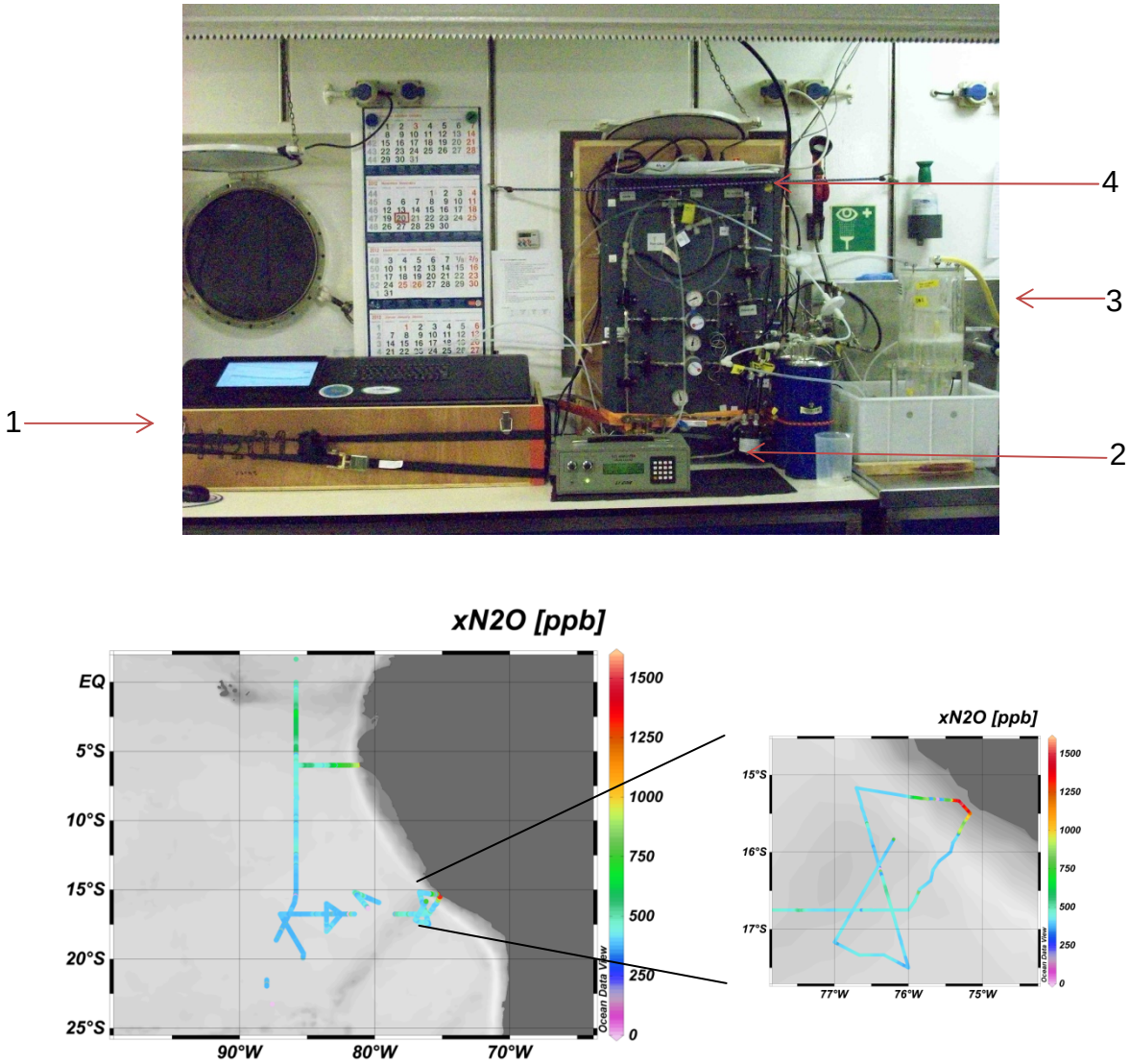

Fig. 5.7 Set up used for underway $N_2O/CO/CO_2$ measurements during the M90 cruise and preliminary results. Upper panel: (1) N_2O/CO Analyzer (2) CO_2 Analyzer (3) Equilibration chamber (4) Manual gas control unit. Lower panel: N_2O molar fraction measured with the DLT-100 analyzer. Supersaturated waters were found along the cruise track with enhanced values towards the coast.

5.2.5 Nitrogen, silicon isotopes

(Patricia Grasse, Martin Frank, Kristin Döring)

Silicon isotopes ($^{28}Si/^{30}Si$) are a powerful tool to investigate the cycling of dissolved silicic acid ($Si(OH)_4$) in the ocean. Upwelling intensity and remineralization of nutrients are directly

driving primary productivity above the OMZ and it is thus crucial to better understand the factors controlling the nutrient distribution. Besides nitrate and phosphate dissolved silicic acid is an important nutrient for diatoms, one of the most abundant primary producers in upwelling areas. Because diatoms preferentially incorporate light isotopes into their valves, the enrichment of heavy isotopes in seawater is an indicator for silicate utilization and the productivity of the diatoms (e.g. De LaRocha et al., 1997). Earlier studies in the Eastern Equatorial Pacific (EEP) during SFB754 cruises M77/3 and M77/4 in January and February 2009 enabled first insights and a first comparison of the dissolved silicon isotope distribution in the water column as well as in the sediments of the study area and present and past nutrient utilization (Ehlert et al., 2012). The silicon isotope distribution ($\delta^{30}Si(OH)_4$) in subsurface waters and within the OMZ of the study area showed that the main factors controlling the Si isotope distribution are different intensities of the dissolution of biogenic silicate ($bSiO_2$) and only partly the mixing of distinct water masses. Dissolution processes are apparently mainly a function of water depth, but bacterial activity, in particular within the OMZs can enhance the $bSiO_2$ dissolution rates. For a better understanding of the remineralization of organic matter and the dissolution of $bSiO_2$ it is necessary to obtain detailed information on the silicon isotope composition of the particulate biogenic opal and the dissolved signature in the same samples, which was not included in the work during the first phase of SFB 754.

Between 1l and 5l of seawater were filtered through 0.65µm Polycarbonate filters. In total 30 stations were sampled during M90 for analysis of profiles of dissolved and particulate Si isotopes. All samples were stored and will be processed and measured at the GEOMAR in Kiel. For additional information about the phytoplankton communities, 0.5 to 1l of seawater were filtered through glasfiber filters for analysis of chlorophyll pigments. Samples for HPLC were sampled at 10 stations with emphasis on the distribution of eddies, which are known to have a large influence on the phytoplankton assemblages.

Radiogenic Neodymium Isotopes and Rare Earth Elements

Large volume water samples were collected for the isotopic characterization of the Rare Earth Element (REE) neodymium ($^{143}Nd/^{144}Nd$) as well as for REE concentration measurements. Due to the fact that water masses acquire their radiogenic Nd isotope signatures through weathering of rocks with particular isotopic compositions, i.e. continental rocks have a lower $^{143}Nd/^{144}Nd$ compared to mantle rocks and young volcanic rocks, the Nd isotope signature fingerprints the origin of water masses (e.g. Frank, 2002). The information from samples that were collected for REE concentration measurements provides further information about continental inputs, particle exchange and scavenging processes, as well as for water mass transport in the ocean. The focus of the sampling was complement the sections taken in 2009 (Grasse et al., 2012) by extending northwards into the Panama Basin and southwards up to 25°S. In addition, the influence of the eddies on the Nd isotope distribution was a goal of the sampling activities.

All water samples were taken from the standard CTD rosette. A total of 50 samples were obtained for neodymium isotope analysis at 11 stations. For each sample, 20 l of seawater were collected in cubitainers from discrete depths. Samples were filtered through a 0.45µm polycarbonate Filter and acidified to a pH of 2 with distilled 10M HCl. To coprecipitate the

neodymium a Fe(III)-chloride solution was added and brought to pH 7-8 using ammonia and the supernatant was siphoned off. The samples will be analyzed at GEOMAR in Kiel.

5.2.6 Dinitrification/anammox ratio

(Cameron Callbeck)

My work onboard the M90 research expedition focused on the subproject B4 of the SFB-754 program. The scope of the B4 addresses nitrogen cycling associated to anammox and denitification (N-loss) but also includes nitrogen fixation as a possible source of new N input into OMZ waters. This work is under the guidance of Gaute Lavik and Marcel Kuypers from the Max Planck Institute in Bremen, Germany with collaborations with Natascha Martogli and Dana Hellemann of GEOMAR.

A CTD rosette equipped with 10L Niskin bottles was used to collect water samples from below the oxycline through the core of the OMZ which ranged from 100 to 500 meters in depth. Sampled stations seen in Figure 5.7 broadly covered the 85°50'W transect as well as three eddies one cyclonic and two anticyclonic along the 16°45'S transect. A total of five depths were chosen per station based on monitored CTD oxygen concentrations. At indicated stations anammox and denitrification 15N-lablelling experiments were performed along with biomass collection on filters for molecular analysis. Incubation substrates for denitrification and anammox were $15NO_2^- + 14NHH_4^+$ and $15NH_4^+ + 14NO_2^-$, respectively. Termination times were at 0, 6, 12, 24 and 48 hours. Rate determinations by mass spectrometry will be done at the MPI-Bremen as well as the analysis of collected biomass by for example quantitative PCR and fluorescence in situ hybridization techniques. Experimental results should be available two to three months following the cruise.

Measuring nitrogen fixation activities was the main task of Natascha Martogli. In support of this work biomass was collected from their $15N_2$ incubation experiments at selected stations seen in Figure 5.8 and will be later analyzed with high resolution nanometer scale secondary ion mass spectrometry (nanoSIMS) and Raman spectrometry at the MPI-Bremen. This will provide a better understanding of the diversity and activity of N_2-fixers on a single cell level in OMZ waters.

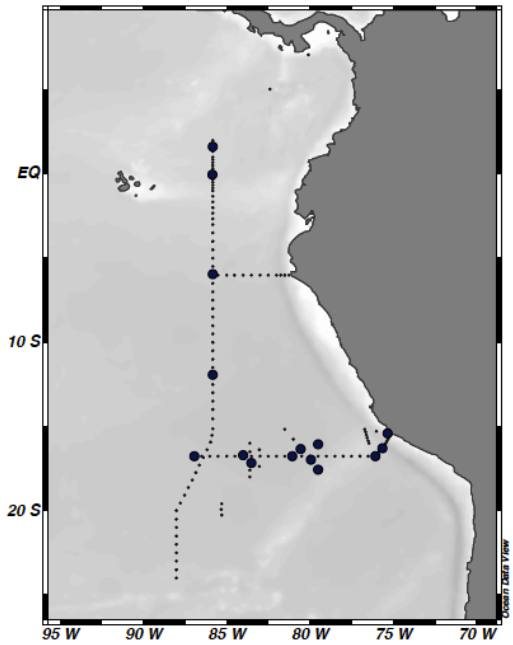

Fig. 5.8 Stations sampled during the M90 cruise highlighted as large black circles.

5.2.7 Nitrogen isotopes and N_2/Ar biogeochemistry

(Chawalit Charoenpong)

The eastern tropical South Pacific (notably off Peru) houses an extensive oxygen minimum zone (OMZ) in its intermediate water. Nearly anoxic conditions found here are favorable for the microbial processes that convert fixed N to N_2 gas ('N-loss'). The Peru OMZ in particular has several unique characteristics including the high concentrations of nitrite (NO_2^-) of more than 10 µmol/kg (Codispoti and Packard, 1980) indicating the potential for multiple N transformation processes (e.g. denitrification, anammox and DNRA). In 2009 (M77/3 and M77/4), a large survey had been conducted and a 'hotspot' for microbially mediated N-loss was found in the coastally-trapped anticyclonic eddy (Altabet et al., 2012). This spatial/temporal heterogeneity in the Peru OMZ calls for an extensive study to assess the impact of the episodic forcings.

Under O_2 deficient condition, NO_3^- is respired (instead of O_2) to remineralize the organic matter and N_2 is yielded as a product in the process called heterotrophic denitrification (NO_3^- => NO_2^- => NO => N_2O => N_2). The consumption of NO_3^- can be assessed by N deficit (N') which is based on the deviation of NO_3^- and NO_2^- from the Redfield ratio with PO_4^{-3} (NH_4^+ omitted as it is known not to accumulate in OMZ's).

$$N' = [NO_3^-] + [NO_2^-] - 16[PO_4^{-3}]$$

The concentrations of the 3 parameters were measured on board and N' were assessed within a day of collection. Alternatively, the N_2 concentrations above saturation (excess N_2) can also be indicative of biological processes that result in N-loss; we collected dissolved gas (DG) samples to evaluate this excess N_2. The latter approach has an advantage as it captures the N_2 produced by both denitrification and its competing process, anammox (NO_2^- + NH_4^+ => N_2 + $2H_2O$). Also, since NO_3^- reduction to NO_2^- causes large isotope effect (Granger, 2006) leaving behind NO_3^- pool with enriched ^{15}N and ^{18}O and corresponding low ^{15}N-N_2, we collected samples for NO_3^-, NO_2^- and N_2 isotopes for analysis on this cruise as well. N_2O, an

intermediate species for both denitrification and nitrification, will be investigated for its isotopic composition. The asymmetry of the N_2O molecule allows the determination of processes that resulted in the N_2O production.

Sample collection and analysis

On M90, samples for $\delta^{15}N$ and $\delta^{18}O$ of NO_3^- and NO_2^-, DG (N_2/Ar and N_2O isotopomers), and underway particulate organic matter (POM) were taken from a total of 160 stations between 7°N and 23° 30'S and from the coast out to 87°W. 38 of which were located within three eddies (2 anticyclonic and 1 cyclonic). No onboard analysis was carried out as all the samples will be shipped back to the School of Marine Sciences and Technology (SMAST), UMass Dartmouth, USA for processing.

Samples for NO_3^- isotopic analysis (collected in 125mL HDPE bottles) were preserved by mild acidification with HCl to pH 2 to 3. Sulfamic acid was also added to remove any NO_2^- present which might interfere with the NO_3^- isotopes. These samples were stored in room temperature until analysis. From the depths where [NO_2^-] were sufficiently high (> 0.5 µmol/kg), samples for NO_2^- isotopic analysis (in 125mL HDPE bottles) were collected. They were frozen at pH 12 to preserve the ^{15}N and ^{18}O signatures.

Back in the lab at SMAST, the NO_3^- samples will be converted to NO_2^- with Cd reduction followed by reaction with azide to produce N_2O (McIlvin and Altabet, 2005) in sealed septum vials. Modification to prevent over-reduction will also be carried out as outlined in Ryabenko et al. (2009). NO_2^- samples will be analyzed in the same manner except with the omission of the Cd step. N_2O gas will be analyzed using a purge-trap interfaced to a GV IsoPrime isotope ratio mass spectrometer (IRMS). POM samples were sampled with a filtration set-up which allowed seawater from underway pumping system to flow through combusted GF/F filters and 5 micron Nitex mesh for size fractionation. Both filters and meshes were kept frozen until analysis which is done using an elemental analyzer coupled to the IRMS.

DG samples were collected using 70mL (N_2/Ar) and 160mL (N_2O isotopomers) septum bottles filled directly from the Niskin bottles. Capping with butyl rubber stoppers were done while all bottles were completely underwater. Great care was taken to ensure absence of any bubbles and samples were poisoned with saturated $HgCl_2$ to stop biological activities. In the lab, high precision N_2/Ar analysis for detection of biogenic N_2 and ^{15}N-N_2 will be determined using on-line gas extraction system coupled to a multicollector IRMS. N_2O isotopomer analysis, on the other hand, will be done using a purge-trap IRMS.

Preliminary results from the nutrient analysis indicated that [NO_2^-] could be larger than 10 µmol/kg in the stations within the eddies. Also, in the center of the cyclonic eddy found closer to the coast (Station 1689), the N' was -48 µmol/kg indicating very active N-loss processes happening in the area. This might present a hotspot for N-loss of comparable or even greater magnitude than previously reported at Station 7 on M77 in Altabet et al. (2012).

5.2.8 PFOS sampling

(Lothar Stramma)

Perfluorooctanesulfonic acid or perfluorooctane sulfonate (PFOS) is a man-made fluorosurfactant and global pollutant. The PFOS levels that have been detected in wildlife are

considered high enough to affect health parameters. It was added to Annex B of Stockholm Convention on Persistent Organic Pollutants in May 2009. Dr. Nobuyoshi Yamashita (AIST Ibaraki, Japan) in cooperation with Dr. Toste Tanhua (GEOMAR Kiel) is investigating the distribution of PFOS in the ocean. One liter water samples were collected at the surface (Kreiselpumpe) at 20 CTD stations and in addition 8 profiles from the CTD-rosette with 5 to 10 samples on each profile were collected (Table 7). These samples were sent to Japan after the cruise for final measurements.

5.3 Biological sampling

5.3.1 Microbial processes

(Dana Hellemann, Natascha Martogli)

5.3.1.1 Dinitrogen (N_2) fixation

Nitrogen is one of the key components of life and therefore a limiting element for biological primary production (Cabello et al., 2004). Atmospheric nitrogen can be made available to the ocean in form of dinitrogen (N2) via nitrogen-fixation which is carried out by prokaryotic organisms known as diazotrophs. This process plays a key role for maintaining biological productivity in the oceans (Capone, 2008; Deutsch et al., 2007) and represents the input mechanism to the marine nitrogen cycle.

In order to investigate nitrogen fixation depth profiles were sampled for analysis of the community structure of N_2-fixing microorganisms (diazotrophs) and their activity and thus the overall input of new nitrogen into the ecosystem.

To examine the direct (O_2) and indirect (N/P) effects of O_2 on rates of N_2-fixation and the functional gene diversity of diazotrophs, 4.5 L samples were taken from the CTD rosette (5 to 9 different depths), fertilized with labeled N_2 ($^{15}N_2$) and incubated for 24 h in either on deck incubators which were continuously filled with ocean surface water and simulated a light attenuation at 15 m water depth or in the cold room with the approximately in situ temperatures using the method developed by Mohr et al. (2010). In order to compare dinitrogen fixation to primary production also ^{13}C bicarbonate was added to the samples alongside the $^{15}N_2$. At the end of each experiment samples for several parameters were taken including DNA/RNA, flow cytometry, nanoSIMS (Cameron Callbeck) and label uptake (^{13}C bicarbonate or glucose and $^{15}N_2$). A total of 17 experiments were performed with a total of 160 samples. Fertilization with ^{13}C glucose was done during three experiments at three selected depths. The samples for dinitrogen fixation were dried at 42 °C for 4 h and stored at room-temperature until analysis in the lab of Ruth Schmitz-Streit using mass spectrometry.

5.3.1.2 Nitrous oxide (N_2O) production along vertical profiles

The oxygen concentrations in the eastern tropical South Pacific (ETSP) are among the lowest concentrations measured in the oceans reaching oxygen concentrations well below 20 µmol L^{-1} (Fuenzalida et al., 2009). This very shallow oxygen minimum is closely coupled to the coastal upwelling along the Peruvian coast enabling the emission of large amounts of

greenhouse gases such as nitrous oxide (N_2O) and carbon dioxide (CO_2) to the atmosphere (Paulmier et al., 2008). Nitrous oxide can be produced both during denitrification and nitrification, but only during the latter it is able to accumulate in the water column and therefore reach the atmosphere. Nevertheless, there is only sparse information available about in situ production of the greenhouse gas N_2O via nitrification, therefore the biological production of nitrous oxide and the thus resulting flux of this potent greenhouse gas from the ocean to the atmosphere was investigated by conducting incubation experiments in either on deck incubators or in the cold room at approximately in situ temperatures.

Small water samples were taken at five to fourteen different depths at a total of 16 stations (200 samples) and incubated for 24 h. Alongside, incubations with the addition of the archaeal inhibitor N1-guanyl-1.7-diaminoheptane (GC7) were conducted to gain an insight into the producing organisms. All samples were taken as triplicates in 50 ml glass vials, closed airtight and conserved with mercury chloride ($HgCl_2$) after the incubations. Measurements and evaluations of N_2O samples will take place in the labs of Hermann Bange and Ruth Schmitz-Streit.

5.3.1.3 DNA/RNA sampling

Samples for DNA/RNA were taken at 12 depths with a total of 34 sampled stations. Small volume (2 L) DNA/RNA samples were filtered through 0.2 µm membrane filters (Millipore, Isopore membrane filters) within a time frame of 20 min directly after collection from the CTD rosette to prevent temperature and light responses in the RNA. Filters were immediately frozen and stored at -80 °C. Alongside 980 µl of these samples were fixed with 20 µl formaldehyde (37 %) and stored at -20 °C for later analysis in the flow meter.

DNA and flow cytometry samples were taken back to the home laboratory in frozen condition for further analysis. In total 560 DNA and 560 flow cytometry samples were taken.

DNA/RNA samples will be analyzed regarding microbial diversity and gene activity in the lab of Ruth Schmitz-Streit. The microbial gene diversity will be analyzed focusing especially on the genes involved in the marine nitrogen cycle. A newly developed microarray will be used to screen for N-cycle genes, results will be verified by quantitative Real Time PCR, sequencing and deep sequencing. To determine the extent to which phylogenetically-related diazotroph ecotypes as well as other microbials involved in the nitrogen cycle are adapted to specific nutrient stoichiometry and O_2 concentrations a metagenomic and metatranscriptomic approach will be used. Also the phylogenetic diversity of 16S rDNA, the *nifH* and the *amoA* genes will be monitored.

The focus of these investigations was on the variability on the transects at 85°50‘W and 16°45‘S.

5.3.2 Squid survey

(Patrick Daniel)

Poleward range shifts of marine species have occurred in conjunction with climate change and warming and a similar phenomenon may be expected in conjunction with OMZ shoaling. The range expansion of the Humboldt squid (Dosidicus gigas) seems to be closely related to the expansion of the OMZ in the Pacific (Gilly et al., 2012). Therefore it was a promising

effort to investigate Humboldt squid occurrence in relation with the large scale oxygen observation in the eastern tropical Pacific during M90.

Squid jigging was performed daily when more than 200 sm off the coast in the evenings and early mornings during CTD casts using rod and reel with traditional squid jigs, ranging in size from 10 - 25 cm. Mantle length (ML) and weight (W) were measured to the nearest 0.1cm and .01 kg, respectively. Sex and maturity were assigned based on Lipinski and Underhill (1995): immature (stages I−II), maturing (III) and mature (IV−V). For all squid, statolith pairs were dissected and stored dry in 3ml centrifuge tubes. In the statolith, a calcareous stone that is part of an equilibrium-related organ, daily growth rings are deposited. When ground and polished into a plane, the rings can be counted and used as a proxy for the age of the individual (Arkhipkin and Shcherbich, 2012). While daily ring deposition has yet to be verified in D. gigas, daily deposition has been verified in other Ommastrephids.

Over the course of the cruise 97 individuals were caught. 84 were identified as Dosidicus gigas, 10 were identified as Sthenoteuthis oualaniensis, the purpleback flying squid, and 3 unknown/inconclusive squid. For individuals of the species Sthenoteuthis o. and individuals that were not positively identified, arm tissue samples were taken and stored in 70% ethanol to be analyzed in the lab. Additionally, for all female squid the presence or absence of spermatorphores around the buccal membrane was noted.

The squid ranged in size from 17.2 to 57.5 (34.5 average) cm ML and from 0.13 to 6.04 (1.29 average) kg weight. Problems arose in landing larger squid due to the height of the deck and the weight of the squid. Because of this, we were unable to land squid larger than 6 kg. A sex ration 1:2.9 males to females were landed over a variety of maturity levels: stage 1 (n =0), stage 2(n=18) stage 3(n=13), stage 4 (n=15) and stage 5 (n = 51). Interesting on several occasions, large immature (stage 2) squid (~3.5kg) were caught at the same station as smaller (23.5) mature (stage 5) squid.

5.4 Underway measurements

(Katharina Höflich, Tina Dippe)

During METEOR cruise M90 several meteorological and oceanographic parameters were measured. Sea surface salinity and temperature were sampled by the ship's Thermosalinograph and by CTD-measurements. Meteorological data include air pressure, wind speed and direction, air temperature, relative humidity and global as well as longwave radiation.

Sea Surface Salinity (SSS) and Sea Surface Temperature (SST) are shown in figure 5.9. Solid lines denote measurements from the ship's Themosalinograph (TSG), red crosses denote uncalibrated CTD-data that was averaged over the upper 3 db of the downcast profiles. Comparison of these two quantities shows that TSG-salinity is on average under-estimated relative to CTD-measurements by -0.0059 ± 0.0010. Note that two CTD-stations yielded strong deviations from TSG-salinities (stations 3 and 118 on Nov 1st and Nov 19th measured 17.071 psu and 28.432 psu compared with 33.141 psu and 35.265 psu obtained from the TSG). These stations were removed from the CTD-dataset. Both primary and secondary TSG-temperatures tend to be slightly higher than CTD-surface temperatures by 0.171 ± 0.021°C and 0.023 ± 0.022°C.

SSTs were found to be relatively high off the Panamesian coast (~ 28°C) and declined roughly to values of approximately 21°C on November 4th (4°S / 85°50°W). A cooling signal due to equatorial upwelling could not be determined. On the 6°S-section, a further SST decrease was associated with coastal upwelling off Peru. Minimum values were as low as 17°C. In heading south, SSTs kept decreasing. In the domain of the (early spring) subtropical gyre, SSTs rarely exceeded 19°C. On the 16°S-section, no prominent changes occurred. SSSs were on average 34.867 psu. Initial values were influenced by coastal waters and could be as low as 28 psu. Upon leaving the central American shelf, SSSs increased and assumed oceanic values until November 4th. The highest values of SSS were found in the domain of the subtropical gyre (35.636 psu). An equator- or ITCZ-related signal could not be extracted from the datat set. Neither could eddies be identified using SST- or SSS-measurements (cf ADCP-, oxygen-, nutrients-measurements).

Meteorological measurements (figures 5.10 and 5.11) included air pressure, air temperature, wind speed, wind direction, humidity and several radiation measures. Air pressure exhibited a typical, diurnal cycle associated with atmospheric tides. Average values were centred on 1013 hPa during the first 10 days of the cruise and increased to values of 1019 hPa when entering the down-welling region on the subtropical flank of the Hadley Cell associated with the subtropical gyre. Air temperature measurements are highly correlated with SST measurements (ρ= 0.969) and exhibit comparable orders of magnitude with water temperatures being higher than air temperatures by 0.95°C on average. Relative humidity was found to be relatively high in tropical regions (85%) and decreased markedly south of 10°S (< 75%). Global Radiation – total solar insulation including backscattered radiation – peaked on average at 800 W/m², with high values associated with relatively cloud-free conditions in the subtropical gyre and lower values in the cloudy regime on the 16°S-section. Longwave radiation – downwelling radiation in the spectrum of terrestrial radiation mainly reflected at clouds, which allows using longwave radiation as a measure of cloudiness – ranged between 440 and 330 W/m². High values of roughly 400 W/m² tended to occur in the rather cloudy tropics, while the subtropics were associated with lower values and fair weather. The time series of UV-radiation is highly correlated with global radiation. Maximum values of 75 W/m² were found in the subtropics, minimum values of 40 W/m² in the cloudy regime of the 16°S-section. Wind was dominated by the trade wind regime throughout the cruise (Figure 5.10). South-easterly wind directions were found in the South Pacific subtropics with wind speeds varying around 7 m/s (Beaufort 4).

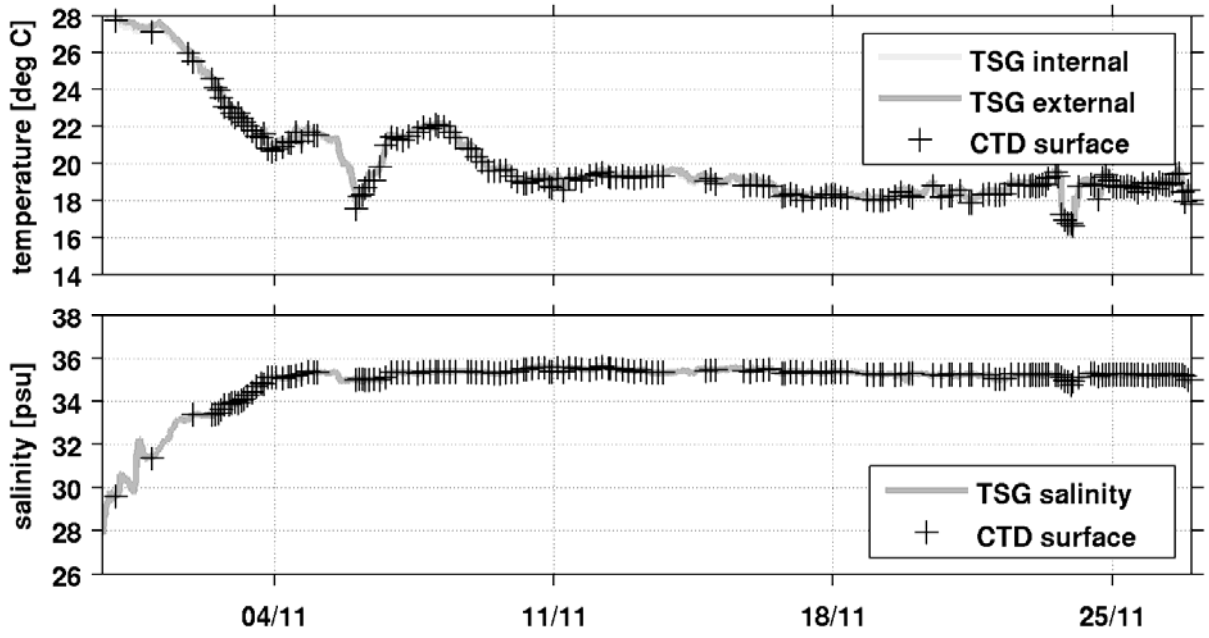

Fig. 5.9 Sea Surface Temperature (top) and Sea Surface Salinity (bottom). For SSTs, both internal and external measurements of the ships Thermosalingraph (TSG) were compared to surface measurements of the CTD-downcasts (average of the upper 3db). TSG-measurements are denoted by solid lines, CTD-measurements by black crosses.

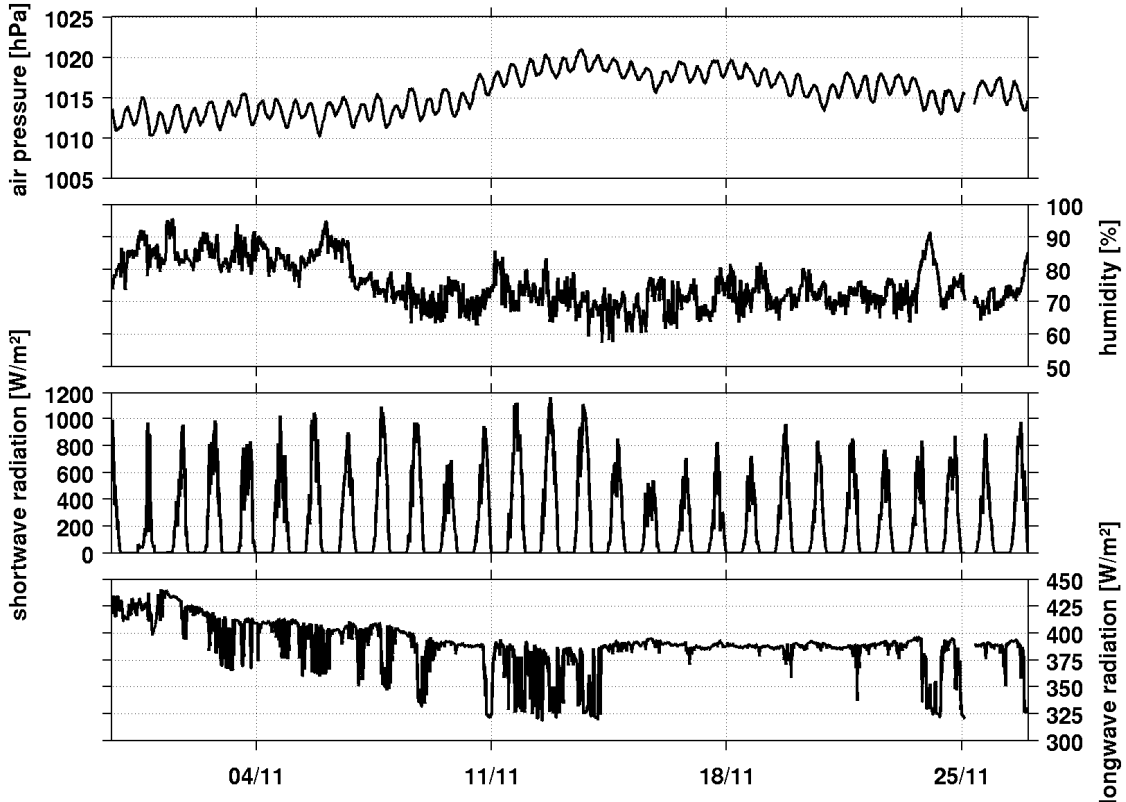

Fig. 5.10: Meteorological measurements. Top: Air pressure in hPa; upper middle: relative humidity in %; lower middle: shortwave (= global) radiation in W/m²; bottom: longwave radiation in W/m². Data was extracted from the DSHIP-database.

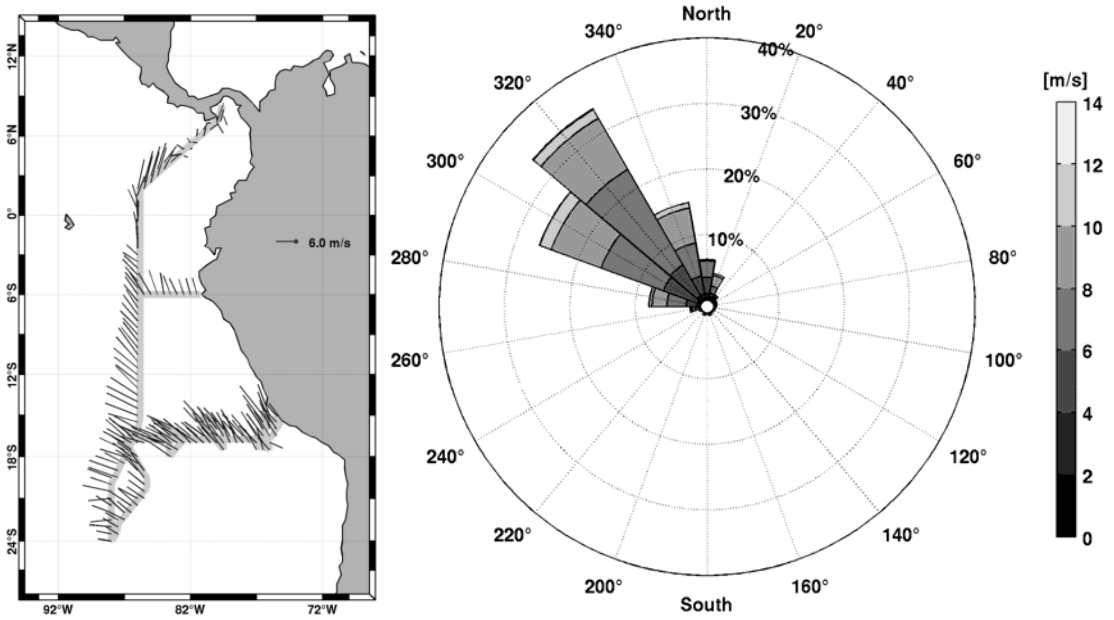

Fig. 5.11: Wind. Left: Ship Track, relative magnitude of wind and meteorological wind direction. Right: Wind histogram. Note that the histogram is taking into account the oceanographic wind direction: It is shown into which direction the wind is blowing, not from which direction it is coming.

6 Ship's Meteorological Station

(Carola Hänsel)

The research vessel "METEOR" lay in the road for bunkering on 27th October 2012. The expedition M90 started with northerly wind about 4 Bft, sea state around 0.5 m, temperatures 28° C and thinning cloud cover the passage through the Panama Channel.

The Innertropical Convergence Zone (ITCZ), which extends from Colombia, the Gulf of Panama and further to westward, partly as a wave across the Pacific, was weather-determining until 1st November.

At first a light and variable wind dominated. Sheet lightning, some showers and on 30th October a thunderstorm was observed during passage ITCZ. With the showers freshening wind 5 Bft with changing wind directions measured, in this thunderstorms wind force 5 to 6 Bft. The thunderstorm was announced with disturbances in the double air pressure wave of the tropics, otherwise to be recognized well.

Then the wind shifted to southwest on the 01st November, from 02nd November mainly south to southeast and reached wind force 4 to 5 Bft, decreasing 3 Bft at times.

With journey to south the research area came onto the southern side of the ITCZ. The temperatures dropped slowly to 20 to 21 degree Celsius. The sea state rose to 1.5 to 2 m, swell direction from southwest.

From the 04th November was the route located on the north flank of a high pressure zone with a south to southwesterly air flow and wind force about 4 Bft.

This high pressure zone extended from a high (1021 hPa) west of the coast of Chile (near 30°S 85°W) to another high (1028 hPa) with centre at 45°S 140°W. This second high was to a

steering pressure system, after it connected with the high close west of Chile on 09th November. An associated ridge (1015 hPa) was extending along the southern coast of Peru along 18°S across the Peru Basin to southwest. The ridge remained almost unchanged until 15th November, after that it expanded a little to north to 12°S and was mainly weather-determining.

The month of November is the last month of "Garúa" time, which is determined from May the weather with some very compact layer of clouds in this region. Fine drizzle or fog is called in Peru "Garúa". This cloud cover was caused by advancing of cold sub polar air. Through this cold air developed an inversion layer, under these clouds formed and also very difficult to dissolve again. This was the reason why, there were only a few hours of sunshine during the expedition.

An inversion is a barrier layer in the atmosphere at a temperature inversion, here temperature increases with altitude. With the daily radio sonde launch was mostly detected the inversion in the region between 1000 and 1500 m, a temperature increasing of about 10 Kelvin.

The research vessel "METEOR" sailed continues to south along 85°50'W from 7th November. Due to the swell going on from southwest the sea state raised to 2.5 to 3 m on 9th and 10th November, in further course sea state was for the most part at 2 to 2.5 m.

The air temperature and water temperature dropped slowly to 18 to 19 degrees Celsius, in the coastal area 16.5 to 17 degrees Celsius from the 8th November. Air temperature was to measure at solar radiations 20 to 21 degrees Celsius.

From 10th to 13th November an upper level trough crossed the research area. Scattered showers occurred in vicinities of the research vessel, on the front of this trough in the morning of 12th and 13th November. An eastwards shifting wind with wind force 5 Bft, gusts 6 Bft was measured in the near of a shower on 12th November.

A new high (1025 hPa) moved from west to the stationary high (1020 hPa) west of Chile and connected with it. The field of research influenced by an associated ridge (1015 hPa), which was still extend from the coastal region further westward along 10°S until the end of the expedition.

A continue southeast- to southerly wind maintained with wind force 4 to 5 Bft, decreased 3 Bft at times. Within at night to 17th and to 24th November the pressure gradient grew in the journey area, because the high intensified and moved temporarily a little to north. The mean wind reached 6 Bft with occasional gusts 7 Bft at times.

The swell was between 1.5 and 2.5 m. It rose temporarily to 3 m due to refreshing wind and southwest- to southerly swell from 22nd to 24th November.

A locally low developed at lee of the hills in the coastal region in the evening of the 26th November.

A fresh, gusty wind from southeast to south about 5 Bft with occasional gusts 7 Bft measured at night to 27th November and in the morning.

During the expedition was to observe a good visibility, partly unusual clear view.

The research vessel "METEOR" arrived at harbour from Callao with gentle southeasterly breeze, sea between 0.5 and 1 m on 28th November 2012.

7 Station List M90

Stat.	CTD	Date	Time	Latitude	Longitude	Depth [m]	Max. p [db]	Comment
ME900/1552-1	001	30.10.12	00:35	07° 04.713' N	80° 04.740' W	2167	2000	1, 5, 8, 10, 11,14, 15s, 16, 17, 18
ME900/1553-1	002	31.10.12	18:03	05° 02.691' N	82° 23.021' W	3055	2956	1, 5, 7, 8, 10, 11, 14, 16, 17, 18
ME900/1554-1	003	01.11.12	20:17	02° 00.036' N	85° 49.978' W	2622	1203	5, 8, 14
ME900/1555-1	004	01..11.12	23:02	01° 40.016' N	85°4 9.998' W	2630	2534	1, 2, 3, 4, 5, 6, 7, 8, 9, 10, 11, 12, 13, 14, 16, 17, 18
ME900/1555-2	005	02.11.12	01:50	01° 40.007' N	85° 50.000' W	2632	252	1, 2, 3, 4, 5, 6, 7, 8, 9, 10, 11, 12, 13, 16, 17, 18
ME900/1556-1	006	02.11.12	04:06	01° 19.999' N	85° 50.003' W	2957	1202	
ME900/1557-1	007	02.11.12	06:46	01° 00.005' N	85° 50.000' W	2796	1202	
ME900/1558-1	008	02.11.12	08:34	00° 50.000' N	85° 49.990' W	2710	1205	
ME900/1559-1	009	02.11.12	10:26	00° 39.945' N	85° 50.073' W	2764	1202	1, 5, 8, 10
ME900/1560-1	010	02.11.12	12:29	00° 30.022' N	85° 50.000' W	2826	1201	14
ME900/1561-1	011	02.11.12	14:20	00° 20.002' N	85° 50.075' W	3052	1201	
ME900/1562-1	012	02.11.12	16:08	00° 10.013' N	85° 49.960' W	2904	1202	14
ME900/1563-1	013	02.11.12	18:54	00° 00.018' N	85° 50.007' W	2929	2832	1, 2, 3, 4, 5, 6, 7, 8, 9, 10, 11, 12, 13, 15, 17
ME900/1563-2	014	02.11.12	21:10	00° 00.002' N	85° 49.975' W	2932	201	1, 2, 3, 4, 5, 6, 7, 8, 9, 10, 11, 12, 13, 15, 17
ME900/1564-1	015	02.11.12	22:36	00° 10.006' S	85° 50.193' W	2728	1204	14
ME900/1565-1	016	03.11.12	00:31	00° 19.974' S	85° 49.980' W	3033	1204	14
ME900/1566-1	017	03.11.12	02:19	00° 29.979' S	85° 50.128' W	2783	1203	
ME900/1567-1	018	03.11.12	04:34	00° 39.996' S	85° 50.134' W	2535	1201	
ME900/1568-1	019	03.11.12	06:06	00° 49.992' S	85° 50.003' W	2421	1203	
ME900/1569-1	020	03.11.12	07:56	00° 59.988' S	85° 50.019' W	2251	1203	1, 7, 10, 13
ME900/1570-1	021	03.11.12	10:39	01° 19.992' S	85° 50.036' W	2466	1201	
ME900/1571-1	022	03.11.12	13:19	01° 39.988' S	85° 50.099' W	2549	1202	14
ME900/1572-1	023	03.11.12	16.10	02° 00.023' S	85° 49.988' W	2779	1202	1, 2, 3, 4, 5, 7, 8, 9, 10, 11, 13, 17
ME900/1572-2	024	03.11.12	17:50	02° 00.022' S	85° 49.985' W	2787	220	1, 2, 3, 4, 5, 7, 8, 9, 10, 11, 12, 13, 15s, 17
ME900/1573-1	025	03.11.12	20:06	02° 20.012' S	85° 50.018' W	3137	1203	
ME900/1574-1	026	03.11.12	22:47	02° 40.001' S	85° 50.006' W	3171	1202	14
Stat.	CTD	Date	Time	Latitude	Longitude	Depth [m]	Max. p [db]	Comment
ME900/1575-1	027	04.11.12	01:25	03° 00.054' S	85° 50.005' W	3235	1205	14
ME900/1576-1	028	04.11.12	04:58	03° 29.993' S	85° 49.987' W	3408	1203	5, 10, 13
ME900/1577-1	029	04.11.12	08:28	04° 00.001' S	85° 49.972' W	3466	1203	1, 2, 3, 4, 5, 7, 8, 9, 10, 11, 13
ME900/1577-2	030	04.11.12	10:15	04° 00.002' S	85° 49.975' W	3462	201	1, 2, 3, 4, 5, 7, 8, 9, 10, 11, 12, 13
ME900/1578-1	031	04.11.12	13:20	04° 30.002' S	85° 49.926' W	3573	1202	14
ME900/1579-1	032	04.11.12	16:47	05° 00.046' S	85° 50.063' W	3838	1201	5, 10, 14, 15
ME900/1580-1	033	04.11.12	20:16	05° 30.005' S	85° 50.013' W	3920	1201	14
ME900/1581-1	034	04.11.12	23:53	05° 59.988' S	85° 50.037' W	4124	1203	1, 2, 3, 4, 5, 6, 7, 8, 9, 10, 11, 13, 15s, 17
ME900/1581-2	035	05.11.12	01:47	05° 59.997' S	85° 50.005' W	4121	201	1, 2, 3, 4, 5, 6, 7, 8, 9, 10, 11, 12, 13, 17
ME900/1582-1	036	06.11.12	01:28	06° 00.022' S	81° 15.508' W	204	198	1,2,3, 4, 5, 8, 9, 10,11, 12, 13, 15s, 17
ME900/1583-1	037	06.11.12	03:20	05° 59.998' S	81° 29.997' W	2437	1201	1, 2, 3, 5, 8, 9, 10, 11, 13, 17
ME900/1583-2	038	06.11.12	05:03	05° 59.996' S	81° 29.997' W	2444	202	1, 2, 3, 5, 8, 9, 10, 11, 12, 13, 17
ME900/1584	039	06.11.12	06:48	06° 00.032' S	81° 45.012' W	4780	1203	5, 9, 10, 11, 12, 17
ME900/1585-1	040	06.11.12	08:54	05° 59.993' S	81° 59.992' W	?	1203	14
ME900/1586-1	041	06.11.12	12:13	06° 00.013' S	82° 30.090 W	4235	1201	1, 4, 5, 9, 10, 11, 12, 17
ME900/1587-1	042	06.11.12	15:29	05° 59.997' S	83° 00.014' W	5430	1201	14
ME900/1588-1	043	06.11.12	19:04	06° 00.007' S	83° 29.997' W	4052	1201	1, 5, 9, 10, 11, 12, 13, 17
ME900/1589-1	044	06.11.12	22:39	06° 00.077' S	84° 00.245' W	4096	1203	14

ME900/1590-1	045	07.11.12	02:05	05° 59.992' S	84° 31.061' W	4188	1201	1, 3, 5, 9, 10
ME900/1591-1	046	07.11.12	05:37	05° 59.993' S	85° 00.021' W	4069	1201	
ME900/1592-1	047	07.11.12	09:03	05° 59.994' S	85° 29.996' W	4135	1201	
ME900/1593-1	048	07.11.12	14:18	06° 29.981' S	85° 50.003' W	4136	1202	1, 3, 14
ME900/1594-1	049	07.11.12	17:56	07° 00.112' S	85° 50.006' W	3990	1202	9, 10, 14
ME900/1595-1	050	07.11.12	21:42	07° 29.929' S	85° 50.034' W	4156	1201	14
ME900/1596-1	051	08.11.12	01:22	07° 59.989' S	85° 49.972' W	4227	1202	1, 3, 5, 7, 9, 10, 11, 13
ME900/1596-2	052	08.11.12	02:56	07° 59.987' S	85° 49.969' W	4225	202	1, 3, 5, 7, 9, 10, 11, 12, 13, 15s
ME900/1597-1	053	08.11.12	06:05	08° 30.012' S	85° 49.978' W	4249	1203	
ME900/1598-1	054	08.11.12	09:34	09° 00.075' S	85° 49.869' W	4266	1202	
ME900/1599-1	055	08.11.12	13:06	09° 29.992' S	85° 50.000' W	4392	1202	1, 8, 10, 14
ME900/1600-1	056	08.11.12	20:46	10° 00.011' S	85° 50.005' W	4430	1202	1, 3, 4, 5, 7, 9, 10, 11, 12, 13, 15
ME900/1600-2	057	08.11.12	22:36	10° 00.011' S	85° 50.008' W	4438	203	1, 3, 4, 5, 7, 9, 10, 11, 12, 13, 15, 20
ME900/1601-1	058	09.11.12	01:42	10° 29.989' S	85° 50.003' W	4341	1202	14
ME900/1602-1	059	09.11.12	05:13	11° 00.022' S	85° 50.138' W	4839	1202	1, 9, 10
ME900/1603-1	060	09.11.12	08:44	11° 29.980' S	85° 49.955' W	4457	1201	
ME900/1604-1	061	09.11.12	12:17	12° 00.004' S	85° 50.012' W	4409	4450	1, 3, 4, 5, 6, 7, 8, 9, 10, 11, 13, 14, 17, 18
ME900/1604-2	062	09.11.12	16:08	11° 59.982' S	85° 50.081' W	4407	301	1, 3, 4, 5, 6, 7, 8, 9, 10, 11, 12, 13, 15s, 17
ME900/1605-1	063	09.11.12	19:12	12° 29.998' S	85 50.024' W	4375	1204	14
ME900/1606-1	064	09.11.12	22:45	12° 59.936' S	85° 50.006' W	4071	1211	9, 10
ME900/1607-1	065	10.11.12	02:27	13° 30.000' S	85° 50.036' W	4706	1201	14
ME900/1608-1	066	10.11.12	06:05	13° 59.979' S	85° 50.054' W	4695	1201	1, 3, 4, 5, 7, 9, 10, 11, 13
ME900/1608-2	067	10.11.12	07:40	13° 59.969' S	85° 50.003' W	4605	201	1, 3, 4, 5, 7, 9, 10,11, 12, 13
ME900/1609-1	068	10.11.12	11:05	14° 31.958' S	85° 50.079' W	4608	1203	
ME900/1610-1	069	10.11.12	15:22	15° 07.976' S	85° 50.015' W	4703	1201	1, 8, 9, 10, 15
ME900/1611-1	070	10.11.12	18:36	15° 31.959' S	85° 53.004' W	4667	1202	14
ME900/1612-1	071	10.11.12	21:35	15° 54.994' S	85° 57.031' W	4661	1202	1, 3, 4, 5, 7, 9, 10, 11, 13
ME900/1612-2	072	10.11.12	23:14	15° 55.000' S	85° 57.003' W	4662	202	1, 3, 4, 5, 7, 9, 10, 11, 12, 13, 15s
ME900/1613-1	073	11.11.12	02:27	16° 21.986' S	86° 09.993' W	4549	1202	14
ME900/1614-1	074	11.11.12	06:07	16° 49.981' S	86° 23.000' W	4508	1202	9, 10
Stat.	CTD	Date	Time	Latitude	Longitude	Depth [m]	Max. p [db]	Comment
ME900/1615-1	075	11.11.12	09:38	17° 16.951' S	86° 37.067' W	4519	1202	
ME900/1616-1	076	11.11.12	13:13	17° 43.971' S	86° 50.983' W	4529	1201	
ME900/1617-1	077	11.11.12	16:51	18° 10.997' S	87° 04.000' W	4401	4419	1, 5, 9, 10, 11, 12, 14, 15s, 17
ME900/1618-1	078	11.11.12	22:00	18° 37.985' S	87° 18.056' W	4429	1202	14
ME900/1619-1	079	12.11.12	01:34	19° 04.989' S	87° 31.016' W	4436	1501	9, 10
ME900/1620-1	080	12.11.12	05:26	19° 32.014' S	87° 45.997' W	4351	1202	
ME900/1621-1	081	12.11.12	09:11	19° 59.996' S	88° 00.032' W	4342	1203	
ME900/1621-2	082	12.11.12	10:08	19° 59.998' S	88° 00.084' W	4348	1202	1, 5, 9, 10, 11, 12, 15
ME900/1622-1	083	12.11.12	13:44	20° 29.989' S	88° 00.014' W	4331	1201	14
ME900/1623-1	084	12.11.12	17:26	20° 50.983' S	88° 00.009' W	4220	1202	9, 10, 14
ME900/1624-1	085	12.11.12	21:00	21° 30.006' S	88° 00.007' W	4225	1202	14
ME900/1625-1	086	13.11.12	00:39	21° 59.967' S	88° 00.036' W	4133	1202	1, 5, 9, 10, 11, 12
ME900/1626-1	087	13.11.12	04:24	22° 29.985' S	88° 00.010' W	4089	1001	
ME900/1627-1	088	13.11.12	07:54	22° 59.978' S	87° 59.976' W	4013	1201	
ME900/1628-1	089	13.11.12	11:27	23° 29.987' S	88° 00.039' W	4121	4156	1, 5, 8, 9, 10, 11, 12, 14, 15, 17, 18
ME900/1628-2	090	13.11.12	14:46	23° 30.000' S	88° 00.006' W	5761	401	1, 5, 8, 9, 10, 11, 12, 16, 16, 17, 18
ME900/1629-1	091	13.11.12	17:52	23° 59.972' S	87° 59.997' W	3969	1202	14
ME900/1630-1	092	14.11.12	19:38	20° 14.967' S	85° 17.003' W	4498	1202	14
ME900/1631-1	093	14.11.12	22:29	19° 55.089' S	85° 19.250' W	4564	2003	1, 5, 10

ME900/1632-1	094	15.11.12	01:40	19° 34.988' S	85° 17.018' W	4879	1202	14
ME900/1633-1	095	15.11.12	18:31	16° 45.032' S	87° 00.034' W	4467	1502	1, 5, 6, 9, 10, 11, 12, 15s
ME900/1634-1	096	15.11.12	22:22	16° 45.186' S	86° 29.983' W	4537	1502	14
ME900/1635-1	097	16.11.12	02:12	16° 45.025' S	85° 59.999' W	4615	1501	14
ME900/1636-1	098	16.11.12	06:07	16° 44.952' S	85° 30.000' W	4575	1502	9, 10
ME900/1637-1	099	16.11.12	09:51	16° 45.060' S	84° 59.988' W	4805	1503	
ME900/1638-1	100	16.11.12	13:37	16° 45.007' S	84° 30.011' W	4608	1500	14
ME900/1639-1	101	16.11.12	17:26	16° 44.984' S	83° 59.992' W	4640	1503	1, 2, 3, 4, 5, 6, 7, 8, 9, 10, 11, 13, 15
ME900/1639-2	102	16.11.12	19:20	16° 44.982' S	83° 59.992' W	4668	252	1, 2, 3, 4, 5, 6, 8, 9, 7, 10, 11, 12, 13, 14, 21
ME900/1640-1	103	16.11.12	22:24	16° 44.968' S	83° 30.088' W	4703	1503	14
ME900/1641-1	104	17.11.12	02:01	16° 44.981' S	82° 59.997' W	5337	1502	15s
ME900/1642-1	105	17.11.12	06:03	16° 44.956' S	82° 30.023' W	5778	1502	1, 3, 9, 10, 18,
ME900/1643-1	106	17.11.12	11:20	17° 21.977' S	83° 01.993' W	4670	1503	9, 10
ME900/1644-1	107	17.11.12	16:45	17° 59.994' S	83° 35.007' W	4439	1502	1, 2, 3, 5, 9, 10, 13, 14, 15s, 17, 21
ME900/1645-1	108	17.11.12	19:57	17° 34.981' S	83° 34.966' W	4366	1501	1, 3, 5, 9, 10, 13, 14
ME900/1646-1	109	17.11.12	23:13	17° 09.936' S	83° 34.879' W	4614	1502	1, 3, 4, 5, 6, 7, 9, 10, 11, 13, 16, 17
ME900/1646-2	110	18.11.12	01:14	17° 09.995' S	83° 34.994' W	5571	201	1, 3, 4, 5, 6, 7, 9, 10, 11, 13, 17, 18, 21
ME900/1647-1	111	18.11.12	05:04	16° 30.019' S	83° 34.958' W	4544	1501	9, 10, 13
ME900/1648-1	112	18.11.12	08:46	15° 59.965' S	83° 35.020' W	5612	1502	1, 9, 13, 17, 21
ME900/1649-1	113	18.11.12	13:41	16° 21.984' S	83° 02.027' W	4925	1501	14, 15s
ME900/1650-1	114	18.11.12	20:47	16° 44.889' S	82° 00.036' W	5042	1501	1, 5, 9, 10, 13, 16, 17, 21
ME900/1651-1	115	19.11.12	00:39	16° 45.035' S	81° 30.008' W	4534	1501	10, 13, 14
ME900/1652-1	116	19.11.12	04:25	16° 44.998' S	80° 59.994' W	4596	1501	1, 2, 3, 5, 6, 7, 8, 9, 10, 11, 13, 16, 17, 21
ME900/1652-2	117	19.11.12	06:18	16° 44.998' S	80° 59.994' W	4588	201	1, 3, 5, 6, 8, 9, 10, 11, 13, 16, 17, 18, 21
ME900/1653-1	118	19.11.12	09:33	16° 45.096' S	80° 30.028' W	4620	1502	
ME900/1654-1	119	19.11.12	13:16	16° 45.017' S	80° 00.036' W	4447	1502	1, 9, 10, 15s
ME900/1655-1	120	19.11.12	17:04	16° 45.042' S	79° 30.066' W	4502	1501	14
ME900/1656-1	121	19.11.12	21:53	15° 59.932' S	79° 30.037' W	4650	1504	1, 5, 6, 7, 9, 10, 11, 13, 16, 17, 21
Stat.	CTD	Date	Time	Latitude	Longitude	Depth [m]	Max. p [db]	Comment
ME900/1656-2	122	19.11.12	23:57	15° 59.995' S	79° 30.005' W	4648	152	1, 5, 6, 7, 9, 10, 11, 13, 16, 17, 21
ME900/1657-1	123	20.11.12	12:03	15° 09.998' S	81° 30.005' W	4740	1502	1, 2, 3, 5, 8, 9, 10 11, 12, 13, 15s
ME900/1658-1	124	20.11.12	17:08	15° 44.996' S	80° 59.960' W	4518	1500	3, 5, 9, 10, 11, 12, 13, 14
ME900/1659-1	125	20.11.12	22:17	16° 19.988' S	80° 30.005' W	4592	1501	1, 3, 4, 4, 5, 7, 9, 10, 11, 13
ME900/1659-2	126	20.11.12	23:50	16° 20.003' S	80° 30.002' W	4588	353	1, 3, 4, 5, 7, 9, 10, 11, 12, 13
ME900/1660-1	127	21.11.12	04:42	16° 54.969' S	80° 00.091' W	4359	1503	3, 5, 6, 9, 10, 11, 12, 13, 17
ME900/1661-1	128	21.11.12	09:58	17° 29.976' S	79° 30.052' W	3713	1504	1, 3, 5, 6, 9, 10, 11, 13, 17
ME900/1661-2	129	21.11.12	11:37	17° 29.986' S	79° 29.998' W	3737	202	1, 3, 5, 6, 9, 10, 11, 12, 13, 17
ME900/1662-1	130	21.11.12	18:21	16° 44.983' S	79° 00.051' W	4215	1502	1, 2, 5, 8, 9, 10, 11, 12, 14, 15s
ME900/1663-1	131	21.11.12	22:05	16° 44.943' S	78° 30.092' W	3573	1503	14
ME900/1664-1	132	22.11.12	01:59	16° 44.984' S	78° 00.060' W	2828	2829	1, 3, 5, 7, 9, 10, 11, 13, 14, 15
ME900/1664-2	133	22.11.12	04:22	16° 44.982' S	78° 00.056' W	3863	353	1, 3, 5, 7, 9, 10, 11, 12, 13, 15
ME900/1665-1	134	22.11.12	07:33	16° 45.034' S	77° 30.058' W	2596	1504	
ME900/1666-1	135	22.11.12	11:16	16° 45.016' S	76° 59.981' W	3242	1502	1, 2, 3, 5, 7, 8, 9, 10, 11, 13, 17
ME900/1666-2	136	22.11.12	12:49	16° 45.002' S	77° 00.000' W	3236	253	1, 2, 3, 5, 8, 9, 10, 11, 12, 13, 17, 18
ME900/1667-1	137	22.11.12	15:52	16° 44.974' S	76° 29.933' W	3582	1502	15s
ME900/1668-1	138	22.11.12	19:21	16° 44.959' S	76° 00.037' W	4136	4156	1, 3, 4, 5, 6, 7, 9, 10, 11, 13, 14, 16, 17, 21
ME900/1668-2	139	22.11.12	22:38	16° 45.003' S	76° 00.021' W	4123	252	1, 3, 4, 5, 6, 7, 9, 10, 11, 13, 16, 17, 21

ME900/1669-1	140	23.11.12	00:07	16° 37.947’ S	75° 54.870’ W	4260	1504	
ME900/1670-1	141	23.11.12	02:04	16° 28.968’ S	75° 50.994’ W	4373	1501	9, 10
ME900/1671-1	142	23.11.12	04:16	16° 21.969’ S	75° 42.041’ W	4245	1502	
ME900/1672-1	143	23.11.12	06:05	16° 13.970’ S	75° 39.966’ W	4414	1501	1, 3, 4, 5, 6, 7, 9, 10, 11, 13, 16, 17, 21
ME900/1673-1	144	23.11.12	08:04	16° 13.995’ S	75^40.012’ W	4407	251	1, 3, 4, 5, 6, 7, 9, 10, 11, 13, 16, 17, 18, 21
ME900/1673-1	145	23.11.12	09:27	16° 06.924’ S	75° 35.039’ W	5297	5359	1, 10, 15s
ME900/1674-1	146	23.11.12	13:48	15° 59.998’ S	75° 26.025’ W	5187	1501	10
ME900/1675-1	147	23.11.12	15:36	15° 52.974’ S	75° 24.039’ W	3758	1502	1, 9,10
ME900/1676-1	148	23.11.12	17:38	15° 45.003’ S	75° 19.019’ W	2084	1501	5, 8,9, 10, 11, 21
ME900/1677-1	149	23.11.12	19:29	15° 37.014’ S	75° 14.994’ W	1217	1205	
ME900/1678-1	150	23.11.12	21:16	15° 29.981’ S	75° 09.998’ W	778	745	
ME900/1679-1	151	23.11.12	23:24	15° 19.833’ S	75° 20.829’ W	199	200	1, 3, 5, 6, 8, 9, 10, 11, 13, 17, 21
ME900/1679-2	152	23.11.12	00:34	15° 19.833’ S	75° 20.829’ W	202	92	1, 3, 5, 6, 8, 9, 10, 11, 13, 15s, 17, 18, 21
ME900/1680-1	153	24.11.12	04:08	15° 16.982’ S	76° 00.019’ W	2914	1501	17
ME900/1681-1	154	24.11.12	08:44	15° 09.967’ S	76° 42.022’ W	3795	1501	1, 5, 9, 10, 11, 12
ME900/1682-1	155	24.11.12	11:10	15° 19.952’ S	76° 39.048’ W	3491	1502	
ME900/1683-1	156	24.11.12	13:26	15° 29.982’ S	76° 36.001’ W	3247	1501	5, 9, 10, 11, 12, 14, 15s, 17
ME900/1684-1	157	24.11.12	15:55	15° 40.001’ S	76° 33.004’ W	3027	1503	
ME900/1685-1	158	24.11.12	18:03	15° 49.988’ S	76° 30.035’ W	3154	1502	5, 9, 10, 11, 12, 14
ME900/1686-1	159	24.11.12	20:11	15° 59.985’ S	76° 27.007’ W	3239	1502	
ME900/1687-1	160	24.11.12	22:19	16° 09.979’ S	76° 24.028’ W	3352	1503	9, 10, 11, 12, 14
ME900/1688-1	161	25.11.12	00:36	16° 20.008’ S	76° 21.030’ W	3619	1502	
ME900/1689-1	162	25.11.12	02:48	16° 29.990’ S	76° 17.988’ W	3735	1501	1, 5, 9, 10, 11, 12, 17
ME900/1690-1	163	25.11.12	05:03	16° 39.994’ S	76° 14.999’ W	3932	1502	
ME900/1691-1	164	25.11.12	07:10	16° 49.981’ S	76° 11.991’ W	4016	1501	
ME900/1692-1	165	25.11.12	09:16	16° 59.993’ S	76° 08.986’ W	4149	1502	5, 9, 10, 11
ME900/1693-1	166	25.11.12	11:28	17° 10.016’ S	76° 05.971’ W	4168	1504	
ME900/1694-1	167	25.11.12	13:36	17° 19.975’ S	76° 02.976’ W	4399	1501	
ME900/1695-1	168	25.11.12	15:44	17° 29.997’ S	76° 00.037’ W	4320	1501	1, 5, 9, 10, 11
ME900/1696-1	169	25.11.12	18:46	17° 20.012’ S	76° 19.926’ W	4101	1200	
Stat.	CTD	Date	Time	Latitude	Longitude	Depth [m]	Max. p [db]	Comment
ME900/1697-1	170	25.11.12	21:26	17° 19.991’ S	76° 39.978’ W	4206	1203	15s
ME900/1698-1	171	26.11.12	00:19	17° 10.018’ S	77° 00.057’ W	3656	1202	5, 9, 10
ME900/1699-1	172	26.11.12	02:21	16° 59.992’ S	76° 54.018’ W	3435	1201	
ME900/1700-1	173	26.11.12	04:19	16° 49.988’ S	76° 48.012’ W	3453	1201	5, 9, 10
ME900/1701-1	174	26.11.12	06:18	16° 39.863’ S	76° 41.917’ W	3347	1204	
ME900/1702-1	175	26.11.12	08:16	16° 30.012’ S	76° 36.045’ W	3266	1202	
ME900/1703-1	176	26.11.12	10:16	16° 19.986’ S	76° 30.023’ W	3361	1202	
ME900/1704-1	177	26.11.12	12:17	16° 09.990’ S	76° 24.028’ W	3333	1203	
ME900/1705-1	178	26.11.12	14:14	15° 59.998’ S	76° 18.015’ W	3283	1201	
ME900/1706-1	179	26.11.12	16:16	15° 49.988’ S	76° 11.007’ W	3605	1202	
ME900/1707-1	180	26.11.12	18:10	15° 39.988’ S	76° 06.037’ W	3137	268	Only downcast to ~ 270 m, problems with the wire on the winch
ME900/1708-1	181	26.11.12	19:47	15° 30.011’ S	76° 00.026’ W	4684	1200	
ME900/1709-1	182	26.11.12	21:45	15° 20.021’ S	75° 54.013’ W	3003	1202	
ME900/1710-1	183	26.11.12	23:41	15° 09.972’ S	75° 48.004’ W	929	906	
ME900/1711-1	184	27.11.12	01:36	14° 59.998’ S	75° 42.007’ W	158	150	

1	Oxygen
2	Fe(II), peroxide
3	N_2O
4	N_2O incubations
5	Dissolved Gas
6	Anammox
7	N_2 fixation
8	Trace metals
9	^{15}N
10	Nutrients
11	pH
12	Chlorophyll
13	DNA
14	Salinity (only for CTD calibration)
15	PFOS (15s: surface only from pump)
16	REEs
17	Si isotopes
18	Nd isotopes
19	Biomass
20	Diatoms
21	Pigments

8 Data and Sample Storage and Availability

The data were collected within the Kiel Sonderforschungsbereich (SFB) 754. In Kiel a joint data management team of GEOMAR and Kiel University organizes and supervises data storage and publication by marine science projects in a webbased multi-user system. In a first phase data are only available to the project user groups. After a three year proprietary time the data management team will publish these data by dissemination to national and international data archives, i.e. the data will be submitted to PANGAEA no later than November, 2015. Digital object identifiers (DOIs) are automatically assigned to data sets archived in the PANGAEA Open Access library making them publically retrievable, citeable and reusable for the future. All metadata are immediately available publically via the following link pointing at the GEOMAR portal (https://portal.geomar.de/metadata/leg/show/316022). In addition the portal provides a single downloadable KML formatted file (https://portal.geomar.de/metadata/leg/kmlexport /316022) which retrieves and combines up-to-date cruise (M90) related information, links to restricted data and to published data for visualization e.g. in GoogleEarth.
Preliminary CTD-data were send already during the cruise M90 to the Coriolis data center for use in “observing the ocean” providing most recent data for modeling approaches.

9 Acknowledgements

We like to thank captain Thomas Wunderlich, his officers and crew of RV METEOR for their support of our measurement program and for creating a very friendly and professional work atmosphere on board. The ship time of METEOR was provided by the German Science Foundation (DFG) within the core program METEOR/MERIAN. Financial support for the different projects carried out during the cruise was mostly provided though the collaborative research program SFB 754 (Climate – Biogeochemical interactions in the tropical Oceans) supported by the German Science Foundation (DFG). We gratefully acknowledge all this support.

10 References

Altabet, M.A., Ryabenko, E., Stramma, L., Wallace, D.W.R., Frank, M., Grasse, P., Lavik, G., 2012. An eddy-stimulated hotspot for fixed nitrogen-loss from the Peru oxygen minimum zone. Biogeosciences, doi: 10.5194/bg-9-1-2012.

Arkhipkin, A., Shcherbich, N., 2012. Thirty years' progress in age determination of squid using statoliths. Journal of the Marine Biological Association of the United Kingdom, 92(6), 1389–1398.

Cabello, P. Roldan, M.D., Moreno-Vivian, C., 2004. Nitrate reduction and the nitrogen cycle in archaea. Microbiology, 150, 3527-3546, doi:10.1099/mic.0.27303-0.

Capone, D., 2008. The marine nitrogen cycle, Microbe, 3(4), 186-192.

Chaigneau, A., Le Texier, M., Eldin, G., Grados, C., Pizarro, O., 2011. Vertical structure of mesoscale eddies in the eastern South Pacific Ocean: A composite analysis from altimetry and Argo. Journal of Geophysical Research, 116, C11025, doi:10.1029/2011JC007134.

Codispoti, L. A., and Packard, T.T., 1980. Denitrification rates in the eastern tropical South Pacific. Journal of Marine Research, 38(3), 453-477.

De LaRocha, C., Brzezinski, M., DeNiro, M. J., 1997. Fractionation of Silicon isotopes by marine diatoms during biogenic silica formation. Geochimica et Cosmochimica Acta, 61, 5051–5056.

Deutsch, C., Sarmiento, J. L., Sigman, D. M., Gruber, N., Dunne, J. P., 2007. Spatial coupling of nitrogen inputs and losses in the ocean, Nature, 445, 163-167, 10.1038/nature05392.

Ehlert, C., Grasse, P., Mollier-Vogel, E., Böschen, T., Franz, J., de Souza, G. F., Reynolds, B.C. Stramma, L., Frank, M., 2012. Factors Controlling the Silicon Isotope Distribution in Waters and Surface Sediments of the Peruvian Coastal Upwelling. Geochimica et Cosmochimica Acta, 99, 128-145.

Frank, M., 2002. Radiogenic isotopes: Tracers of past ocean circulation and erosional input. Reviews of Geophysics, 40, 1-37, doi: 10.1029/2000RG00034.

Fuenzalida, R., Schneider, W., Garcés-Vargas, J., Bravo, L., Lange, C., 2009. Vertical and horizontal extension of the oxygen minimum zone in the eastern South Pacific Ocean. Deep Sea Research Part II: Topical Studies in Oceanography, 56, 992-1003.

Gilly, W.F., Beman, J.M., Litvin, S.Y., Robinson, B.H., 2012. Oceanographic and biological effects of shoaling of the oxygen minimum zone. Annual Review of Marine Sciences, doi: 10.1146/annurev-marine-120710-100849.

Granger, J., Sigman, D. M., Lehmann, M. F., and Tortell, P. D., 2006. Nitrogen and oxygen isotope fractionation during dissimilatory nitrate reduction by denitrifying bacteria. Limnology and Oceanography, 53, 2533–2545.

Grasse, P., Stichel, T., Stumpf, R., Stramma, L., Frank, M., 2012. The distribution of neodymium isotopes and concentrations in the Eastern Equatorial Pacific Water mass advection versus particle exchange. Earth And Planetary Science Letters, 353-354(C), 198–207.

Lipinski, M., Underhill, L., 1955. Sexual maturation in squid: Quantum or continuum? South African Journal of Mar.ine Sciences, 15, 207−223.

McIlvin, M. R. and Altabet, M. A., 2005. Chemical conversion of nitrate and nitrite to nitrous oxide fornitrogen and oxygen isotopic analysis in freshwater and seawater. Analytical Chemistry, 77, 5589–5595.

Mohr, W., Grosskopf, T., Wallace, D. W. R., LaRoche, J., 2010. Methodological underestimation of oceanic nitrogen fixation rates, PLoS One, 5, e12583.

Paulmier, A., Ruiz-Pino, D., and Garcon, V., 2008. The oxygen minimum zone (OMZ) off Chile as intense source of CO2 and N2O. Continental Shelf Research, 28, 2746-2756, 10.1016/j.csr.2008.09.012.

Ryabenko, E., Altabet, M. A., Wallace, D. W. R., 2009. Effect of chloride on the chemical conversion of nitrate to nitrous oxide for 15N analysis. Limnology and Oceanography, 7, 545–552.

Stramma, L., Johnson, G.C., Sprintall, J., Mohrholz, V., 2008. Expanding oxygen-minimum zones in the tropical oceans. Science 320, 655-658.

Stramma, L., Prince, E.D., Schmidtko, S., Luo, J., Hoolihan, J.P., Visbeck, M., Wallace, D.W.R., Brandt, P., Körtzinger, A., 2012. Expansion of oxygen minimum zones may reduce available habitat for tropical pelagic fishes. Nature Climate Change 2, 33-37.

Thamdrup, B., Dalsgaard, T., Revsbech, N.P., 2012. Widespread functional anoxia in the oxygen minimum zone of the Eastern South Pacific. Deep-Sea Research I,65, 36-45.

Winkler, L.W., 1888. Die Bestimmung des im Wasser gelösten Sauerstoffes. Berichte der deutschen chemischen Gesellschaft, 21(2), 2843-2854.